

University of Nevada, Reno

**MODELING DEFICIT IRRIGATION STRATEGIES FOR ALFALFA IN NORTHERN
NEVADA**

A thesis submitted in partial fulfillment of the
requirements for the degree of **Master of
Science in Environmental Sciences and
Health**

by

KHUSHI

Dr. Manuel Alejandro Andrade-Rodriguez /Thesis Advisor

December, 2025

Copyright by FNU Khushi 2025
All Rights Reserved



THE GRADUATE SCHOOL

We recommend that the thesis
prepared under our supervision by

FNU KHUSHI

entitled

**Modeling Deficit Irrigation Strategies for Alfalfa in
Northern Nevada**

be accepted in partial fulfillment of the
requirements for the degree of

MASTER OF SCIENCE

Manuel A. Andrade-Rodriguez, Ph.D.
Advisor

Juan K. Q. Solomon, Ph.D.
Committee Member

Thomas Parchman, Ph.D., Post Doctoral
Graduate School Representative

Markus Kemmelmeier, Ph.D., Dean
Graduate School

December, 2025

Abstract

Water scarcity in the western United States has intensified the need for irrigation strategies that sustain alfalfa yield while conserving limited water resources. This study aimed to calibrate and evaluate the Cropping System Model (CROPGRO) Perennial Forage Model to simulate alfalfa growth and yield under full and deficit irrigation management in northern Nevada. A comprehensive, multi-year (2021-2023) and multi-harvest dataset was developed from a field experiment conducted at the University of Nevada, Reno's Valley Road Field Laboratory, using two alfalfa cultivars and three irrigation treatments. The dataset integrates detailed observations of weather, soil, irrigation, crop growth, and yield. A sensitivity analysis using a one-at-a-time approach identified three parameters as the most influential in driving the variability of simulated yield. These parameters were optimized using a two-stage genetic algorithm approach implemented in the Python programming language. The calibrated model achieved good performance with a Root Mean Square Error (RMSE) of 715 kg/ha, a coefficient of determination (R^2) of 0.88, and a normalized Root Mean Square Error (nRMSE) of 16.5 % for the first two growing seasons (2021-2022) that were used for calibration, and acceptable accuracy for the third growing season (2023) (RMSE = 1695 kg/ha, R^2 = 0.92, nRMSE = 39.5 %) that was used to evaluate the calibrated model. The model successfully reproduced multi-harvest yield patterns and irrigation responses, demonstrating its capability to simulate alfalfa performance under arid and semi-arid conditions. This work lays the foundation for developing a regional Alfalfa yield forecasting tool that can be used to optimize irrigation scheduling and enhance water-use efficiency.

Keywords: Alfalfa, Deficit irrigation, Crop growth model, Decision Support System for Agrotechnology Transfer, Perennial forage model, Calibration

Dedication

*"A river cuts through rock not because of its power,
but because of its persistence."*

(James N. Watkins)

Acknowledgement

I want to begin by expressing my deepest gratitude to my advisor, Dr. Manuel A. Andrade-Rodriguez, for his constant support and guidance throughout my graduate studies. From the very beginning, he encouraged me to explore my own ideas while helping me stay focused on what mattered most. His patience, encouragement, and thoughtful advice have been invaluable. He has always taken the time to provide clear and helpful feedback, which pushed me to think critically and improve my work. I am especially thankful for his steady presence and willingness to guide me through both the exciting and the difficult parts of this research.

I am also very grateful to my committee members, Dr. Juan K. Q. Solomon and Dr. Thomas Parchman, for their thoughtful suggestions, guidance, and feedback. Their input has greatly improved the quality of this work and helped me grow as a researcher.

I owe special thanks to my family for their endless love and encouragement. My parents, Dr. Mamta Rani and Mr. Satish Kumar, have always been my biggest source of strength. They have stood beside me in every step of my life, encouraging me to work hard and never give up. Without their constant support and sacrifices, this accomplishment would not have been possible. I also want to thank my brother, Nishith, for his support, which has given me the courage to follow my goals with confidence to finish this journey.

To my colleagues in the Precision Irrigation Management (PRIMA) Lab, Dr. Uriel Cholula Rivera and Mahipal Reddy Ramireddy, I want to extend my sincere thanks. It has been a pleasure working alongside you. Your collaboration, teamwork, and friendship made the long days of research more enjoyable, and I am grateful for the knowledge and experiences we shared. I also want to thank Scott Huber, Senior Assistant Director of NAES, for his tremendous help with the

field operations. His dedication and practical support ensured that our research could move forward smoothly.

I would also like to acknowledge the institutions and programs that made this work possible. This project benefited greatly from the support of the Nevada Agricultural Experiment Station (NAES) and the College of Agriculture, Biotechnology & Natural Resources of the University of Nevada, Reno. I am also grateful for the financial support provided by the U.S. Department of Agriculture, National Institute of Food and Agriculture, Data Science for Food and Agricultural Systems program under Award No. 2023-67022-40041. Without these resources and support, completing this research would not have been possible. I am also thankful for the opportunity to attend the DSSAT 2025 International Training Program in Griffin, Georgia, which enhanced my understanding of crop modeling and strengthened the foundation for this research.

Finally, I would like to thank all my friends and the many people I have met during this time. Each of you, in your own way, has made this journey brighter and easier. I am grateful for every moment and for the sense of community that made my stay so meaningful.

Table of Contents

Abstract	i
Dedication	ii
Acknowledgement.....	iii
List of Figures	viii
List of Tables.....	viii
1. Introduction.....	1
1.1. Background/ Motivation	1
1.2. Problem Statement	2
1.3. Research Gaps.....	2
1.4. Objectives of the Study.....	3
1.5. Significance of the Study	3
2. Literature Review.....	4
2.1. Alfalfa and Its Uses.....	4
2.2. Irrigation Management Strategies for Alfalfa Production	5
2.3. Crop Growth Simulation Models for Alfalfa.....	5
2.4. CSM-CROPGRO-PFM for Alfalfa.....	10
2.5. Sensitivity Analysis, Calibration, and Evaluation of Alfalfa Crop Models.....	13
2.6 Genetic Algorithms (GA)	16
2.7 Hypothesis.....	18

3.	Materials and Methods.....	19
3.1.	Overview of Previous Alfalfa Field Experiment	19
3.2.	Contents of the Dataset	21
3.2.1.	Weather Data	21
3.2.2.	Soil Data.....	22
3.2.3.	Soil-Water Data	23
3.2.4.	Irrigation Management.....	23
3.2.5.	Alfalfa Harvesting Dates and Hay Yield for Each Harvest	24
3.2.6.	Crop Development Indicators	24
3.2.7.	Biomass.....	24
3.3.	Model Inputs	24
3.3.1.	Meteorological Data.....	24
3.3.2.	Soil Data.....	25
3.3.3.	Alfalfa Field Management	26
3.4.	Model Sensitivity Analysis, Calibration, and Evaluation.....	29
3.5.	Performance Statistics.....	32
4.	Result and Discussion.....	34
4.1.	Sensitivity Analysis	34
4.2.	Model Calibration and Validation	35

4.2.1.	Stage 1: General Calibration.....	35
4.2.2	Stage 2: Cultivar-Specific Calibration.....	38
4.2.3	Evaluation Year - 2023.....	40
4.2.4	Treatment-Specific Model Performance.....	44
4.2.5	Cut-Wise Yield Patterns.....	46
4.2.6	Overall Performance.....	49
5	Limitations of the Study.....	52
6	Future Work.....	53
7	Conclusions.....	53
	References.....	55
	Appendix.....	62

List of Tables

Table 1. Summary of recent studies using process-based alfalfa growth models to estimate above-ground biomass and their reported statistical indicators of accuracy: the coefficient of correlation (R^2), the normalized Root Mean Square Error (nRMSE), the Nash-Sutcliffe model efficiency coefficient (EF), and Willmott's index of agreement (d)	9
Table 2. Previous studies using CSM-CROPGRO-PFM to model alfalfa under diverse environmental conditions, highlighting fall dormancy (FD) ratings of alfalfa cultivars, growing seasons (calendar year in which the crop grows/ regrows and is harvested), treatments, irrigation systems used, number of harvests per year, sites, and associated climate types	12
Table 3. Overview of key CSM-CROPGRO-PFM parameters identified in previous studies to simulate alfalfa performance across different regions, highlighting the most sensitive parameters affecting yield and the calibration approaches followed in each study	14
Table 4. Soil physical and hydraulic properties by depth, including texture (clay and silt content), organic carbon, field capacity (FC), permanent wilting point (PWP), bulk density, soil root growth factor, and saturated water content in the experimental field	26
Table 5. Harvest dates of alfalfa during the 2021-2023 growing seasons	27
Table 6. Summary of sensitivity analysis for key cultivar and ecotype parameters	33
Table 7. Comparison of parameter values before, in stage 1, and in stage 2 calibration	37
Table 8. Treatment-wise model performance for 2021, 2022, and 2023 after Stage 2 calibration	44
Table 9. Comparison of model performance across calibration stages and years	50

List of Figures

Figure 1. Schematic representation of the GA workflow with its components and operators	18
Figure 2. Experimental layout showing three irrigation treatments (full irrigation 100%, mild deficit irrigation 80%, and moderate deficit irrigation 60%) and two alfalfa cultivars (Ladak II and Stratica). A yellow circle inside a plot indicates that a soil moisture sensing station was placed in the middle of the plot.....	20
Figure 3. Mean monthly averages of temperature and precipitation recorded in Reno, NV (WRCC, 2025) during the growth period in 2021, 2022, and 2023	21
Figure 4. Workflow of model calibration and validation process for alfalfa yield simulation using the CSM-CROPGRO-PFM	30
Figure 5. Workflow of the Genetic Algorithm calibration process integrated with DSSAT	31
Figure 6. Simulated versus observed alfalfa yield for the 2021 and 2022 growing seasons under full and deficit irrigation treatments after the first stage of calibration. Each point (2021) or cross (2022) represents an individual cut across both cultivars (Ladak II and Stratica). The 1:1 dashed red line indicates perfect agreement between observed and simulated yields	36
Figure 7. Convergence curve of Genetic Algorithm (GA) during the first calibration stage	37
Figure 8. Simulated versus observed alfalfa yield for the 2021 and 2022 growing seasons after cultivar-specific GA calibration, showing improved alignment across irrigation treatments and cultivars with respect to the general calibration (Stage 1)	39
Figure 9. Simulated versus observed alfalfa yields for the 2023 evaluation year after 2 stages of GA calibration. Each point (2023) represents an individual cut across both cultivars (Ladak II and Stratica) and three irrigation treatments. The 1:1 dashed red line indicates perfect agreement between observed and simulated yields	42

Figure 10. Comparison of overall average observed and simulated seasonal alfalfa yields across irrigation treatments (100 %, 80 %, and 60 % FI) and cultivars (Ladak II and Stratica) during 2021-2023. Where 1 is 100% + Stratica, 2 is 80% + Stratica, 3 is 60% + Stratica, 4 is 100% + Ladak II, 5 is 80% + Ladak II, and 6 is 60% + Ladak II 45

Figure 11. Observed and simulated cut-wise yields under 1=100 %, 2=80 %, and 3=60 % irrigation treatments for years 2021, 2022, and 2023 across both cultivars after 2 stages of GA calibration. Here, C1 is the first cut, C2 is the second cut, C3 is the third cut, and C4 is the fourth cut 47

Figure 12. Simulated versus observed yields for the years 2021, 2022, and 2023 after 2 stages of GA calibration. The 1:1 dashed red line indicates perfect agreement between observed and simulated yields 49

1. Introduction

1.1. Background/ Motivation

Alfalfa (*Medicago sativa* L.) is the third most valuable field crop in the United States, generating approximately \$8.7 billion annually across 23 million acres of cultivation (USDA-NASS, 2023). Nearly 40% of this production occurs in the western states (Putnam et al., 2020), where it is essential to the dairy and livestock industries. In Nevada, alfalfa is the leading cash crop, yielding over 1.15 million tons per year on about 0.24 million acres (Nevada Annual Bulletin, 2023). Its high productivity, however, comes with high water demands. In arid and semi-arid regions, such as Nevada, meeting alfalfa's evapotranspiration (ET) requirement depends on substantial irrigation (Lindenmayer et al., 2011). Water scarcity in the region is driven by climate change, prolonged drought, and groundwater depletion, and is intensifying by unprecedented declines in Colorado River and Lake Mead levels (Colorado River Commission, 2024; Saito et al., 2022). These challenges emphasize the urgent need for irrigation strategies that sustain yield while conserving limited water resources.

Deficit irrigation (DI), which is applying less water than the full evapotranspiration requirement of the crop, offers one such approach to water conservation. Unlike Full Irrigation (FI), where soil water depleted within the root zone is fully replenished, DI replenishes only a fraction of that water. Research shows that DI can reduce water use while maintaining acceptable yields (Carter et al., 2013; Cholula et al., 2022), though its success depends on deficit severity, the level of drought tolerance of a crop, the growth stage(s) when the crop experiences water stress, and environmental conditions. Excessive water stress during sensitive periods can sharply reduce yields, undermining water savings (Li et al., 2023).

To guide irrigation decisions effectively, farmers need tools that predict how different water management strategies influence seasonal yield and forage quality. Crop growth models can fulfil this role by integrating soil, climate, management, genetic, and pest factors to simulate daily plant growth and development (Malik & Dechmi, 2019; Quintero et al., 2023). Such models have proven valuable for irrigation management, yield forecasting, and precision agriculture, enabling scenario testing without the time and cost of repeated field trials (Zhao et al., 2024).

1.2. Problem Statement

Despite their potential, crop growth models have been limited in their application to alfalfa cultivated in arid and semi-arid environments. Available datasets required to develop alfalfa growth models for these regions are often incomplete, lacking the multi-year, multi-harvest, and high-resolution data needed for calibration and validation. Studies rarely evaluate multiple irrigation strategies, cultivar-specific responses, and environmental variability within alfalfa (Malik et al., 2018; Jing et al., 2020; Boote et al., 2022; Raes et al., 2023). Model performance under northern Nevada's severe weather conditions remains poorly understood. Without comprehensive, region-specific calibration, predictive accuracy is limited, reducing the crop growth model's practical utility for balancing water efficiency with sustained productivity (Wang et al., 2024).

1.3. Research Gaps

1. Limited application of crop growth models to estimate alfalfa hay yield under arid and semi-arid conditions.
2. Scarcity of multi-year datasets that can be used for calibration and validation of alfalfa crop growth models in northern Nevada.

3. Limited information about alfalfa cultivar-specific responses to DI strategies under the highly variable climatic conditions typical of northern Nevada.

1.4. Objectives of the Study

1. Develop a comprehensive, multi-year, multi-cultivar, region-specific database characterizing the effects of water stress on alfalfa grown in northern Nevada.
2. Use the database to calibrate an alfalfa crop growth model fitted to the environmental and management conditions of northern Nevada.
3. Evaluate the model's ability to simulate alfalfa growth and yield under FI and DI management strategies across two alfalfa cultivars.

1.5. Significance of the Study

Results obtained from this study will support the future development of an open-source Alfalfa Yield Forecasting Tool (YFT), which will be aimed at promoting sustainable water management in the arid Western U.S. The YFT will help producers make informed, real-time irrigation decisions by simulating yield responses to various irrigation schedules and identifying optimal strategies to maximize seasonal yield while staying within water quotas. As part of this broader effort, this research focuses on the calibration and evaluation of a crop growth model under northern Nevada-specific conditions, using multi-year and multi-harvest field data collected from an experiment applying FI and DI treatments to different alfalfa cultivars. The calibrated model will not only enhance the accuracy of alfalfa hay yield forecasting in northern Nevada, but it can also be used in the future to assess the effects that different irrigation management strategies and/or the effects of a shifting climate can have on alfalfa production in the region. The development of

an alfalfa crop growth model can thus assist the identification of actionable takeaways for improving water use efficiency in northern Nevada.

2. Literature Review

2.1. Alfalfa and Its Uses

Alfalfa, known as the "queen of forages," is a perennial legume from the family *Papilionoideae*, native to the Mediterranean mountain forests of southwestern Asia (Zhou et al., 2024). The crop's historical and cultural significance is reflected in its name, derived from the Arabic term *Al-Fasfasa*, meaning "the father of all plants" (Lamb et al., 2006). Globally, alfalfa is valued for its high forage yield, superior fiber quality, and rich protein content, making it a cornerstone in livestock feed production (Fink et al., 2022). Incorporation into animal diets has been shown to enhance growth and reproductive performance, resulting in increased meat and milk production (Yang et al., 2024). Its deep and extensive root system enables it to tolerate arid and semi-arid conditions, maintaining growth even under moderate water stress (Cholula et al., 2022; Ma et al., 2021). This adaptability allows alfalfa to be cultivated on marginal lands with limited water availability.

As a versatile forage crop, alfalfa can be harvested multiple times per year, depending on climate and management practices. In Nevada, the growing period of alfalfa is from May to October, with four harvests typically obtained in each season, with the first harvest usually producing the highest yield (Cholula et al., 2024). The crop is utilized in various forms as hay, silage, or pellets, and is widely traded as a global agricultural commodity (Mullins et al., 2009). However, its high-water demand compared to many other crops presents a significant production challenge, particularly in water-limited regions like Nevada (Putnam et al., 2020). This challenge

signifies the importance of optimizing irrigation management strategies to sustain high yields while improving crop water productivity.

2.2. Irrigation Management Strategies for Alfalfa Production

Deficit irrigation (DI) is widely studied as a water-saving practice, involving the deliberate application of less water than the crop's full ET requirement. For alfalfa, DI has demonstrated potential to reduce water use while maintaining economically viable yields (Carter et al., 2013; Cholula et al., 2022; Karam et al., 2011). The success of DI, however, depends on multiple factors, including the severity and timing of water deficits, environmental conditions, and the crop's tolerance to water stress (Li et al., 2023; Sanderson et al., 1994; Teshome et al., 2023). While mild to moderate DI during less sensitive growth stages may result in minimal yield loss, severe or poorly timed deficits, particularly during regrowth and peak biomass accumulation periods, can significantly reduce both yield and forage quality (Fereris & Soriano, 2006). This trade-off highlights the significance of developing irrigation scheduling methods that take into account the variable sensitivity to water stress experienced by alfalfa during its different growth stages.

2.3. Crop Growth Simulation Models for Alfalfa

Crop models are defined as mathematical algorithms that simulate crop growth and development by integrating quantitative data about weather, soil characteristics, and crop management, allowing for predictions and assessments of various agricultural scenarios (Chapagain et al., 2022). Irrigation scheduling methods supported by crop growth models can be used to identify water-sensitive growth stages when water stress should be minimized or avoided to optimize water savings without triggering unacceptable yield losses.

Broadly, crop growth models fall into two categories: **process-based models** and **data-driven models**. Process-based models simulate plant growth using underlying physiological and biophysical principles of a crop. They are not only used to predict yield but also to investigate how environmental factors regulate plant physiological processes and how these interactions influence growth, development, and yield (Zhang et al., 2023). In contrast, data-driven models rely on large datasets to identify patterns and relationships as they learn from historical data to make predictions without explicitly simulating the biological processes involved (Zumwald et al., 2021, Quintero et al., 2023).

Over the past five decades, several process-based crop growth simulation models have been developed or adapted specifically to describe and predict the growth, development, and yield of alfalfa under diverse environmental and management conditions. These models vary in their complexity, input data requirements, and capacity to capture physiological processes unique to perennial forage systems. **SIMED** (Holt et al., 1975; Schreiber et al., 1978) was the first alfalfa-specific model that simulated dry matter partitioning among leaves, stems, and roots. While it incorporated many core physiological processes, it did not simulate regrowth after cutting or non-structural carbohydrate dynamics, the two critical drivers of perennial forage productivity. **ALSIM** and **ALSIM1** (Fick, 1981) addressed this gap by introducing subroutines for bud development and regrowth following harvest. The first version used monthly average temperature and solar radiation and assumed no soil water or fertility limitations, thus predicting potential rather than actual yields. **ALFALFA 1.4** (Denison & Loomis, 1989) provided a more detailed physiological approach, simulating growth at the tissue and organ level, including leaves, stems, internodes, crowns, taproots, and fibrous roots. However, it offered limited capacity to integrate environmental stress factors. **ALF2LP** (Bourgeois, 1990) expanded **ALSIM**'s framework by including total non-

structural carbohydrate reserves for spring regrowth, daily biomass accumulation for different plant parts, and the effect of plant age as a limiting factor on radiation use efficiency. Hence, improved multi-harvest simulation capabilities. **Integrated Farm System Model (IFSM)** (Jégo et al., 2015; Rotz et al., 2012) has been adapted for alfalfa-timothy mixtures, demonstrating good predictive performance for yield and neutral detergent fiber content, a parameter for forage quality. However, its assumption of optimal drainage and fertility, along with a post-harvest biomass reset to zero, limits its accuracy for simulating realistic alfalfa regrowth processes. **STICS** (Brisson et al., 1998; Strullu et al., 2020), adapted for alfalfa, is a generic crop model that estimates biomass using radiation use efficiency but lacks perennial-specific processes such as drought tolerance mechanisms and ammonium volatilization, restricting its accuracy under water-limited conditions. This model was tested in France, another major alfalfa producer (Strullu et al., 2020). **CropSyst** (Confalonieri & Bechini, 2004; Stöckle & Nelson, 1999), a process-based model, has been calibrated for alfalfa in rotation systems with corn for silage production, but it does not explicitly simulate crown and root regrowth or fully represent carbohydrate reserve mobilization, limiting its suitability for stand-alone perennial modeling.

Overall, most of these models focus primarily on potential production, which is the maximum possible yield, and have limitations in simulating the full range of physiological and morphological processes in alfalfa. More recent process-based growth models available for alfalfa include:

1. **APSIM (Agricultural Production Systems sIMulator)** (Keating et al., 2003), which has been tested for alfalfa in Australia, Argentina (Ojeda et al., 2016), New Zealand (Moot et al., 2015), and Northeast China (Peng et al., 2022) (Table 1). While highly flexible, its alfalfa simulations require substantial location-specific calibration for accurate performance. As

explained by Moot et al. (2015), understanding the underlying physiological processes for different growing conditions, cultivars, and environments remains essential to use this model.

2. **AquaCrop** (Raes et al., 2009; Steduto et al., 2009) was recently adapted for alfalfa and evaluated in Belgium, Turkey, and Canada (Raes et al., 2023) (Table 1). It focuses on water productivity under different irrigation regimes. Although initial results are promising (Raes et al., 2023), the newly incorporated regrowth algorithms for perennial crops require further testing across diverse regions.
3. **Cropping System Model-CROPGRO-Perennial Forage Model (CSM-CROPGRO-PFM)** within the Decision Support System for Agrotechnology Transfer (DSSAT) software (Hoogenboom et al., 2019) is among the most specialized modules available for simulating alfalfa growth. This model provides detailed descriptions of plant phenology, reserve compound utilization, growth of reserve organs, and regrowth initiation after defoliation (including stubble mass and leaf proportion), which are essential for accurately representing perennial forage systems (Rymph et al., 2004). CSM-CROPGRO-PFM has been evaluated in northeast Spain (Malik et al., 2018), eastern Canada (Jing et al., 2020), and China (Miao et al., 2025) to simulate biomass production and assess irrigation strategies (Table 1). However, calibration and validation using region-specific datasets are still needed (Malik et al., 2018), particularly under extreme weather and diverse management conditions.

Table 1: Summary of recent studies using process-based alfalfa growth models to estimate above-ground biomass and their reported statistical indicators of accuracy: the coefficient of correlation (R^2), the normalized Root Mean Square Error (nRMSE), the Nash-Sutcliffe model efficiency coefficient (EF), and Willmott's index of agreement (d).

Crop Model	Country/region of study	Statistical Indicators				References
		R^2	nRMSE	EF	d	
CSM-CROPGRO-PFM/DSSAT-FORAGES Alfalfa-model	Northern Spain	-	26%	-	0.75	Malik et al. (2018)
	Eastern Canada	-	24%	0.48	0.86	Jing et al. (2020)
	Arizona, Montana	Unpublished Results				Boote et al. (2022)
	Inner Mongolia, China	0.94	4.72%	-	-	Lv et al. (2025)
	Northern China	>0.85	<11%	-	-	Miao et al. (2024)
	Northwest China	0.89	5.88 %	-	-	Miao et al. (2025)
APSIM-Lucerne	Argentine Pampas, SE Australia	0.87	-	0.86	-	Ojeda et al. (2016)
	China	0.81	13%	-	-	Peng et al. (2022)
	New Zealand	-	38%	-	-	Moot et al. (2015)
AquaCrop	Belgium, Turkey, Ottawa	0.97	11%	0.97	0.99	Raes et al. (2023)
STICS	France	0.92	36 %	0.70	-	Strullu et al. (2020)

2.4. CSM-CROPGRO-PFM for Alfalfa

This study evaluated the **CSM-CROPGRO-PFM**, released with **DSSAT v4.8** (available at dssat.net), to simulate alfalfa growth under Nevada's arid and semi-arid conditions. CSM-CROPGRO-PFM is one of the most detailed process-based models available to simulate perennial forages because it accounts for multiple harvests, seasonal regrowth, and environmental stress responses (Malik et al., 2018). The model simulates daily crop growth processes, including herbage accumulation, forage protein content, and regrowth across successive harvests and years. A key strength is its representation of perennating storage organs (crown and taproot), which contain carbohydrate and nitrogen reserves that sustain regrowth even after complete shoot removal (e.g., cutting or frost-induced leaf loss). The mobilization and replenishment of these reserves are explicitly modelled, enabling a realistic simulation of alfalfa's regrowth dynamics under intensive harvest management (Boote et al., 2022).

CSM-CROPGRO-PFM also takes into account physiological mechanisms critical to simulate alfalfa adaptation to different environments, management practices, etc., including:

- Fall dormancy (FD), which is defined as the reduction in shoot growth in the autumn due to decreasing temperatures and daylength (Teuber et al., 1998), and freeze thresholds, which govern regrowth potential and winter survival under cold conditions.
- Dynamic biomass partitioning, adjusted by growth stage and photoperiod.
- Storage pool dynamics, regulating the balance between reserve mobilization for regrowth and refilling during favourable growth periods.
- Management sensitivity, where repeated or aggressive defoliation can reduce recovery potential (Jing et al., 2020).

By adjusting model parameters, CSM-CROPGRO-PFM allows simulation of genetic and cultivar variation, including differences among dormancy classes, cultivars, and their interactions with contrasting environments. Previous studies have applied CSM-CROPGRO-PFM for alfalfa under a range of climatic and management conditions (Table 2), highlighting its flexibility and relevance for diverse agro-ecosystems. Given its ability to represent key physiological processes, regrowth cycles, and cultivar-specific responses, CSM-CROPGRO-PFM is well-suited for testing DI strategies in northern Nevada with different cultivars. However, accurate application requires region-specific calibration and validation, particularly for local cultivars and under the region's extreme climate variability. This research, therefore, focuses on adapting and validating CSM-CROPGRO-PFM using a multi-year, multi-harvest dataset collected from a previous experiment conducted in northern Nevada.

Table 2: Previous studies using CSM-CROPGRO-PFM to model alfalfa under diverse environmental conditions, highlighting fall dormancy (FD) ratings of alfalfa cultivars, growing seasons (calendar year in which the crop grows/ regrows and is harvested), treatments, irrigation systems used, number of harvests per year, sites, and associated climate types.

Paper References	Alfalfa Cultivar (Fall Dormancy)	Growing Seasons	Treatments tested	Number of Harvests/ Year	Irrigation System	Sites tested	Climate type
Malik et al. (2018)	Aragon (FD = 7)	8	Model adapted from <i>Bracharia brizantha</i>	5-6	Sprinkler Irrigation	The Ebro Valley in Northern Spain	Mediterranean semiarid climate
Jing et al. (2020)	Apica (FD=4); Oneida VR (FD=3)	23	Impacts of climate change	Vary with site (1-4)	N/A	6 sites in Eastern Canada	Humid Continental and Subarctic climate
Boote et al. (2022)	Rugged (FD = 3), Cisco II (FD = 6), CUF 101 (FD = 9)	N/A	Different Fall dormancy classes	2 in Montana and 7 in Arizona	N/A	Arizona, Montana	Arid and continental climate
Lv et al. (2025)	Algonquin (FD = 1)	2	Seven Levels of Irrigation Quota, 6 Nitrogen levels	3	Basin Irrigation	Dengkou County in Inner Mongolia	Temperate continental monsoon climate
Miao et al. (2024)	Grassland No.2 (FD = N/A)	2	Four Levels of Irrigation Quota	2	Drip Irrigation	Inner Mongolia	Temperate semi-arid continental monsoon
Miao et al. (2025)	Algonquin (FD = 1)	2	Dry year and Wet year	2	Subsurface Drip Irrigation	Wuchuan County in Northwestern China	Temperate continental monsoon

2.5 Sensitivity Analysis, Calibration, and Evaluation of Alfalfa Crop Models

To adapt a process-based alfalfa crop growth model to a specific region, the first step is to identify key parameters that affect crop performance indicators of interest, such as crop yield, through sensitivity analysis. Sensitivity analysis assesses the impact of variations in input parameters, such as genetic coefficients or environmental factors, on model outputs (Attia et al., 2021). This step is necessary for identifying which physiological, environmental, or management-related variables have the greatest impact on simulated productivity. Once key parameters are identified, the next step is calibration. Calibration involves adjusting genetic, environmental, and management-related coefficients to minimize discrepancies between observed and simulated crop yield values (Akhavizadegans et al., 2021). This process ensures that the model accurately represents local production conditions. For example, in northern Nevada, alfalfa yield is influenced by limited water availability, the number of harvests, cultivar-specific responses, and unusually low or high air temperatures during the winter or summer, respectively (Quintero et al., 2023). Table 3 summarizes applications of CSM-CROPGRO-PFM across diverse regions, highlighting the sensitivity analysis parameters that most strongly influenced yield and the calibration methods employed in each case.

Table 3: Overview of key CSM-CROPGRO-PFM parameters identified in previous studies to simulate alfalfa performance across different regions, highlighting the most sensitive parameters affecting yield and the calibration approaches followed in each study.

Study	Malik et al. (2018)	Jing et al. (2020)	Boote et al. (2022)	Lv et al. (2025)	Miao et al. (2024)	Miao et al. (2025)
Calibration Method	Bayesian optimization, inverse modeling techniques, and Literature	Manual (process understanding)	Results Not Published	Trial and error (outcome comparison)	Trial and error (outcome comparison)	Using statistical indicators
Cultivar file parameters (describe genetic traits specific to an individual cultivar within a crop species [Lamsal et al., 2017])						
Parameters *	Calibrated Value	Calibrated Value	Calibrated Value	Calibrated Value	Calibrated Value	Calibrated Value
CSDL	-	-	-	10	10.5	10.5
PPSEN	-	-	-	0.5	0.2	0.2
EM-FL	-	-	-	17.2	21.5	21.5
FL-SH	-	-	-	5.5	6.7	6.7
FL-SD	-	-	-	11.3	-	12.6
SD-PM	-	-	-	30	33.5	33.5
FL-LF	-	-	-	14	16	16
LFMAX	1.40	1.34 (FD=3), 1.32 (FD=4)	-	1.9	2.4	2.5
SLAVR	280	240	-	200	300	290
SIZLF	-	-	-	5	5	5

Ecotype file parameters (describe the broader physiological and environmental adaptation characteristics shared among cultivars within a species. For example, temperature, solar radiation, photoperiod [Lamsal et al., 2017])						
RDRMT	0.421	0.421 (FD=3), 0.500 (FD=4)	0.500 (FD=3), 0.32, (FD=6), 0.140 (FD=9)	-	-	-
RMRMM	-	0.95	-	-	-	-

* Definitions of these parameters are available in Appendix Table 1

The primary approaches used for calibrating crop model parameters include traditional trial-and-error methods, statistical optimization techniques, and intelligent optimization algorithms (Ma et al., 2021). Although the manual and trial-and-error approach remains widely used, it heavily depends on the modeler’s experience and subjective judgment, often making the calibration process cumbersome, time-consuming, and prone to human bias. With advancements in computational methods, automatic and intelligent optimization algorithms have gained attention for their superior efficiency and accuracy in parameter estimation (Wang et al., 2023). Among these, Genetic Algorithms (GA) have emerged as a particularly robust technique capable of efficiently exploring complex, non-linear parameter spaces (Colpan et al., 2021; Cimino et.al., 2023). Inspired by the principles of natural selection, GA iteratively evolves parameter combinations to minimize discrepancies between simulated and observed values, making it especially effective for model calibration tasks, such as those performed within DSSAT (Wang et al., 2023). Following calibration, model evaluation is conducted to assess the accuracy and reliability of the calibrated model parameters under independent conditions.

2.6 Genetic Algorithms (GA)

A GA is a global optimization algorithm based on the principle of survival of the fittest. This heuristic optimization technique is inspired by natural selection and genetics. It belongs to the family of evolutionary algorithms and is designed to search for near-optimal solutions to complex, non-linear problems that are difficult to solve using conventional methods (Holland, 1992). GAs mimic biological evolution through mechanisms such as selection, crossover (recombination), and mutation, which iteratively improve a population of candidate solutions according to their fitness values (Melanie, 1996). In a GA, each potential solution is represented as a sequence of variables known as genes, collectively forming a chromosome. A group of chromosomes constitutes a population, and each population represents a generation. The algorithm begins by generating an initial population of solutions randomly or based on prior knowledge. Each chromosome is evaluated using a predefined objective (fitness) function, which quantifies how well it performs relative to the optimization goal (Figure 1). The evolutionary process then proceeds through successive generations, applying three main operators:

1. Selection - Chooses the fittest individuals (parents) to contribute genetic material to the next generation.
2. Crossover - Combines pairs of parent chromosomes to create new offspring, for exploration of new solution spaces.
3. Mutation - Introduces small random variations to maintain diversity and prevent premature convergence (Melanie, 1996).

Over multiple generations, the population evolves toward an optimal or near-optimal solution. The process terminates when one of the following criteria is met.

1. A predefined number of generations is reached
2. The improvement between successive generations becomes negligible, or
3. A satisfactory fitness level is achieved.

Due to its stochastic nature, the GA may yield different solutions across runs. However, these solutions typically converge near the global optimum (Whitley, 1994). GAs have been widely used in model calibration and regression-based prediction problems because of their ability to efficiently explore complex, multidimensional parameter spaces and avoid local minima (Khanmohammadi et al., 2021).

In the context of crop growth modelling using DSSAT, GA has been more frequently used in optimizing management strategies, such as irrigation and fertilization scheduling, than in calibrating model parameters. For example, Wang et al. (2023) integrated GA with DSSAT to optimize maize irrigation schedules under variable climatic conditions, while Bai et al. (2021; 2022) applied a GA-DSSAT framework to simultaneously optimize irrigation and fertilizer management. Earlier, Pabico, Hoogenboom, and McClendon (1999) demonstrated the potential of GA for estimating cultivar coefficients in crop models and emphasized its ability to navigate multi-dimensional and non-linear parameter spaces more efficiently than traditional calibration methods. Although GA-based genetic calibration within DSSAT is less common compared to using calibration tools embedded in DSSAT, such as GLUE (Generalized Likelihood Uncertainty Estimation) or PEST (Parameter ESTimation), these tools have not yet been adapted or validated for alfalfa parameter calibration. Given this gap, GA presents a promising alternative due to its reliability, flexibility, and capacity to handle complex, multi-objective calibrations.

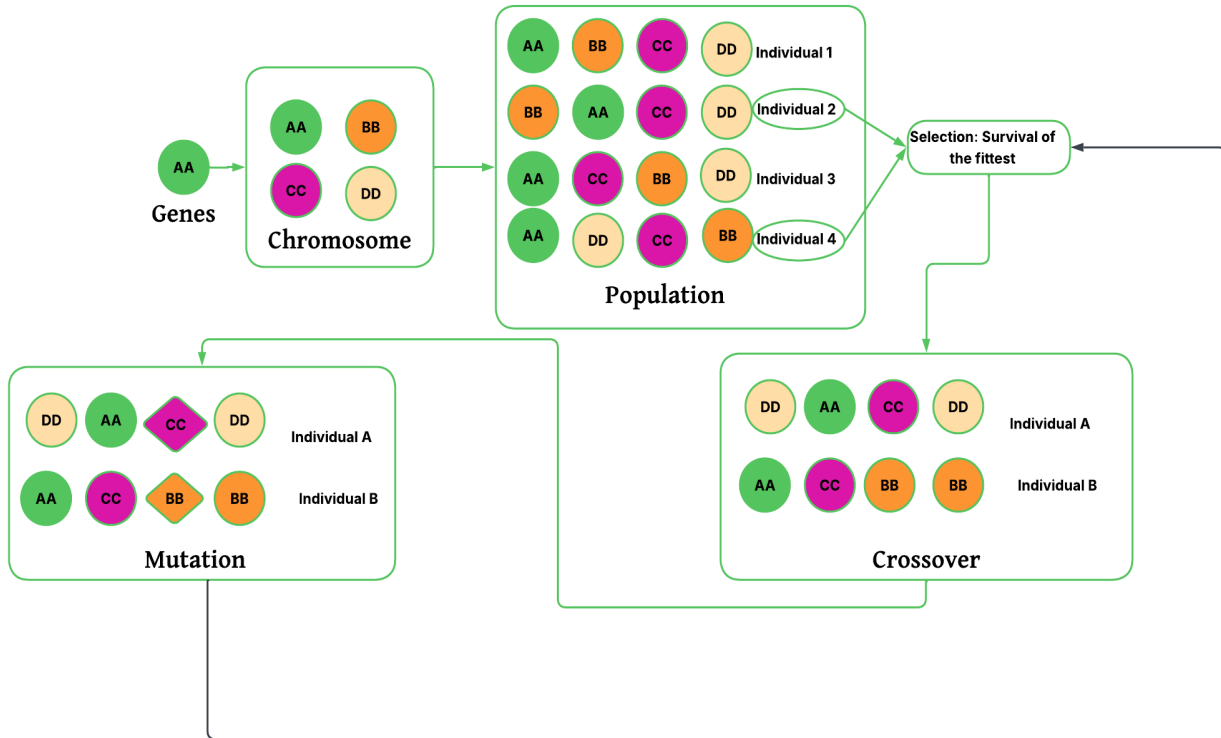


Figure 1: Schematic representation of the GA workflow with its components and operators.

2.7 Hypothesis

H1: The CSM-CROPGRO-PFM model, when calibrated with multi-year and multi-harvest field data from northern Nevada, will simulate alfalfa growth and yield in the region across different cultivars and irrigation treatments with satisfactory accuracy.

H2: The model will capture key agronomic patterns, such as higher yields in the first harvest and decreasing yields in subsequent cuts, as well as yield reductions under increasing water stress.

H3: Calibrating the most sensitive parameters with the genetic algorithm will significantly improve the model's performance metrics.

3. Materials and Methods

A comprehensive database was created for this study using data collected from a previous experiment conducted in northern Nevada, integrating multi-year and multi-harvest field observations collected under Full Irrigation (FI) and Deficit Irrigation (DI) treatments across two alfalfa cultivars. The database includes detailed records of weather variables, soil physical and hydraulic properties, irrigation schedules, crop growth measurements, and yield data. This dataset serves as a foundation for simulating, calibrating, and validating the CSM-CROPGRO-PFM within the DSSAT framework.

3.1. Overview of Previous Alfalfa Field Experiment

The previous alfalfa experiment was conducted at the Valley Road Field Laboratory (VRFL) of the University of Nevada, Reno (39°32'29.42" N, 119°48'18.09" W; elevation 1,370 m) (Figure 2). The experiment was carried out during the summer growing seasons of 2021, 2022, and 2023 using a surface drip irrigation system. The local climate in Reno is classified as semi-arid, characterized by cold winters and hot, dry summers. The average annual precipitation and snowfall are 186.7 mm and 530.9 mm, respectively, with most precipitation occurring between January and February. The mean annual reference evapotranspiration (ET_o) is approximately 1,435 mm, and the mean annual temperature is 12.8 °C. Figure 3 shows the monthly average temperature and precipitation during the 2021-2023 study period. The soil at the experimental site is classified as a Fleishmann gravelly clay loam with 2-4% slopes (Soil Survey Staff et al., 2025). The experiment aimed to evaluate the response of two alfalfa cultivars to three irrigation treatments: FI, Mild DI (80% of FI), and Moderate DI (60% of FI) under northern Nevada conditions. The field was established in the fall of 2020, as it is customary in the region, with two commercial alfalfa

cultivars: ‘Ladak II’ (Great Basin Seed, Ephraim, UT), marketed as drought-tolerant, and ‘Stratica’ (CROPLAN, Arden Hills, MN), marketed as high-yielding. Additional experimental details are provided in Cholula-Rivera (2025).

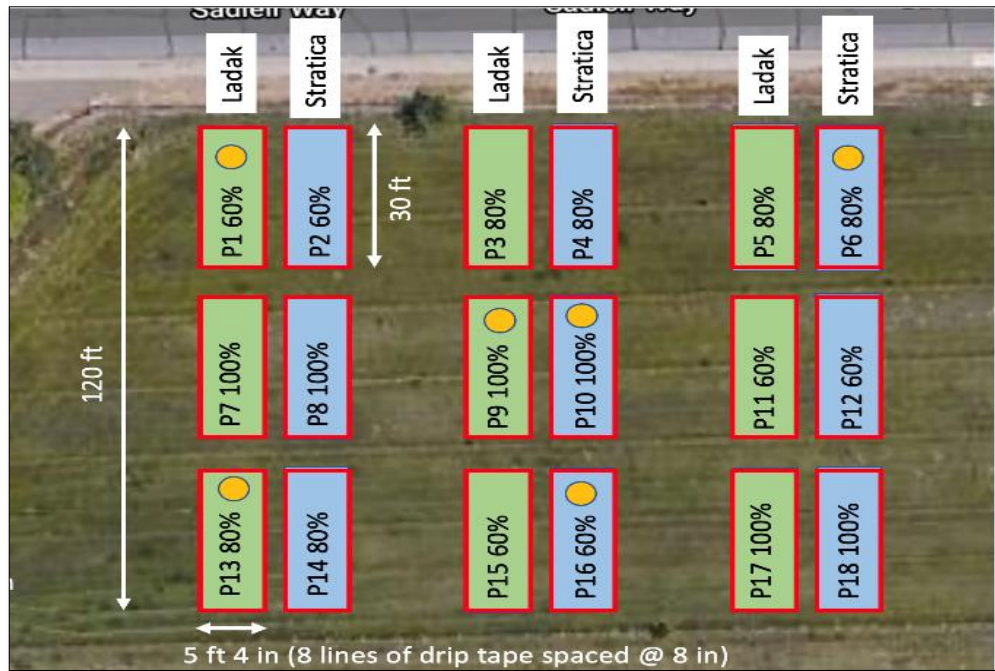


Figure 2: Experimental layout showing three irrigation treatments (full irrigation 100%, mild deficit irrigation 80%, and moderate deficit irrigation 60%) and two alfalfa cultivars (Ladak II and Stratica). A yellow circle inside a plot indicates that a soil moisture sensing station was placed in the middle of the plot (Cholula Rivera, 2025).

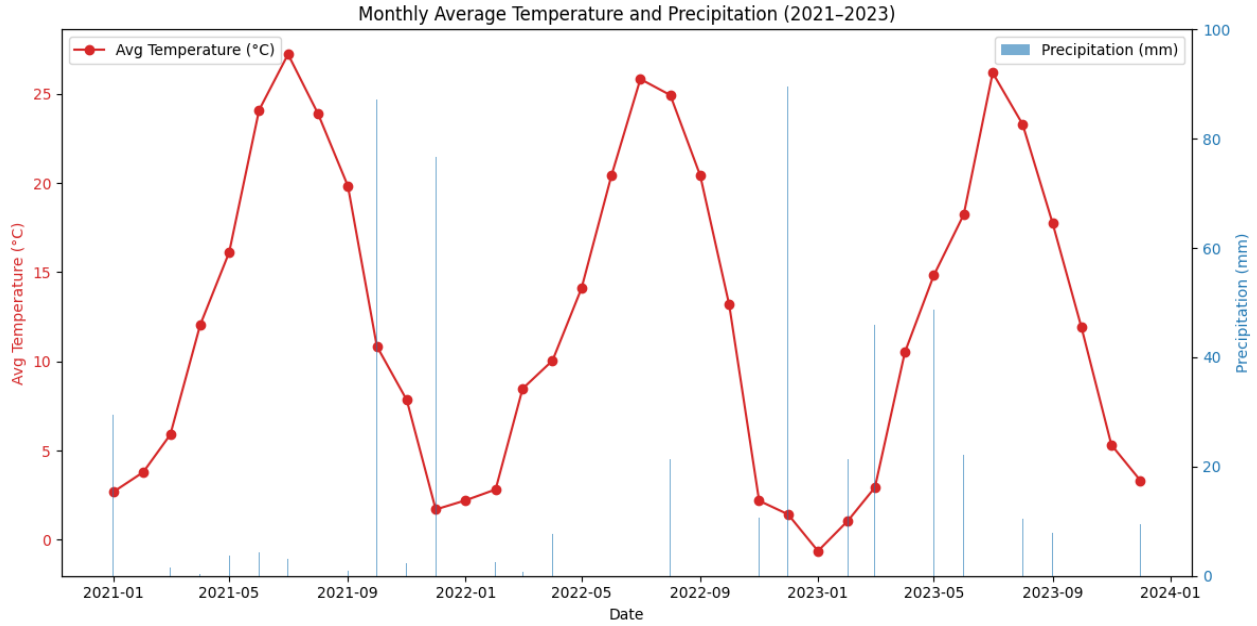


Figure 3: Monthly average air temperature and cumulative precipitation recorded in Reno, NV (WRCC, 2025) during 2021, 2022, and 2023.

3.2. Contents of the Dataset

The dataset contains information that is accessible to most crop managers in the western U.S., such as weather data, irrigation amounts and irrigation dates, harvesting dates, and alfalfa hay yield obtained from each harvest, plus additional information not typically available to most crop managers, such as soil water content (%), Leaf Area Index (LAI), plant height (cm), fresh biomass obtained in between harvests (kg/ha). This additional information will enable us to assess whether incorporating these detailed measurements into the model enhances its accuracy and reliability.

3.2.1. Weather Data

Throughout the growing season, daily and hourly weather data were collected from a weather station located near the VRFL, approximately 250 m from the experimental plots. The data

recorded by this station are publicly available through the Western Regional Climate Center (WRCC, 2025). The following meteorological parameters were included in the weather dataset:

1. Total Solar Radiation (MJ/m²/day)
2. Average Wind Speed (m/s)
3. Average Air Temperature (degrees Celsius)
4. Total Precipitation (mm)
5. Relative Humidity (%)
6. Reference Evapotranspiration (mm)

3.2.2. Soil Data

Soil information includes general site and surface information as well as soil profile characteristics. This data was obtained from the USDA-NRCS's Web Soil Survey (Soil Survey Staff et al., 2025) and/or by testing soil samples in a laboratory. The following site and soil information were included in the soil dataset:

1. Location of experimental site
 - Latitude
 - Longitude
 - Elevation
2. Soil Surface information
 - Soil Series
 - Soil Classification
 - Soil Color
3. Soil Profile data for each soil horizon

- Sand, Silt, and clay (%)
 - Soil Texture
 - Field Capacity, Permanent Wilting Point, and Available Water Capacity
4. Soil Chemical Properties (According to the soil analysis report)
- Organic Matter (%)
 - Individual Macronutrients (ppm)
 - Individual Micronutrients (ppm)
 - Soil pH
 - Cation Exchange Capacity (meq/100g)
 - Percent Cation Saturation
 - Soluble Salts (dS/m)

3.2.3. Soil-Water Data

Soil water sensors based on Time Domain Reflectometry (TDR) were used to measure soil volumetric water content (%) at multiple depths within the soil profile. Hourly water content measurements were obtained using six soil water sensing stations consisting of three TDRs (model 315H, Acclima, Meridian, ID) each, buried at depths of 20, 60, and 90 cm (Figure 2).

3.2.4. Irrigation Management

A surface drip irrigation system was used throughout the experiment to apply FI and DI treatments. The dataset includes detailed records of each irrigation event, including the date and the amount of water applied (mm) to individual plots. This irrigation management data allows for the evaluation of different water application strategies.

3.2.5. Alfalfa Harvesting Dates and Hay Yield for Each Harvest

The harvesting dates of alfalfa, along with the corresponding dry hay yield (in kg/ha) obtained from each plot during each harvest, were included in the dataset. Dry hay yield is the main variable to be simulated by the CSM-CROPGRO-PFM.

3.2.6. Crop Development Indicators

Agronomic indicators of crop development provide details on the development and progression of the alfalfa crop over time (Yang et al., 2024). Biweekly measurements of plant height and LAI were recorded throughout the experiment across all three growing seasons.

3.2.7. Biomass

The dataset included fresh and dry biomass measurements (kg/ha) collected on a biweekly basis during the 2021-2023 growing seasons. These data provide valuable information on the productivity and growth dynamics of alfalfa over time, supporting the assessment of seasonal yield patterns.

The generation of this database lays the foundation for the next objective of this study, which aims to evaluate the CSM-CROPGRO-PFM's ability to simulate the growth and yield of alfalfa cultivated in northern Nevada.

3.3. Model Inputs

3.3.1. Meteorological Data

Meteorological data were incorporated into the model using the WeatherMan utility tool available within DSSAT, which converts raw weather observations into a standardized text file

format required for model execution (Jones et al., 2003). The file requires essential daily variables such as precipitation, maximum and minimum air temperature, solar radiation, relative humidity, and wind speed, which are necessary to drive the crop growth simulations.

3.3.2. Soil Data

Soil data were entered into the model using the SBuild (Soil Build) utility tool within DSSAT. The SBuild program is a soil data preparation tool that enables users to create or modify soil profile files by combining measured and estimated soil properties into the standardized format required for model simulations (Jones et al., 2003). The soil information used for modeling was obtained from the USDA-NRCS Web Soil Survey (Soil Survey Staff et al., 2025), supplemented by field soil sampling to determine the primary soil physical characteristics and initial conditions necessary for model inputs (Table 4).

In Table 4, the Soil Root Growth Factor (SRGF), which represents the relative root length distribution (ranging from 0.00 to 1.00) within each soil layer, and the saturated water content were calculated using the SBuild program based on measured soil characteristics, including layer thickness, depth, clay, silt, coarse fraction, and organic carbon content. The field capacity (FC) and permanent wilting point (PWP) values were initially obtained from the NRCS Web Soil Survey and later refined through model simulations to minimize discrepancies between observed and simulated soil moisture data. The FC and PWP values presented in Table 4 represent the final adjusted values used for modeling. The initial soil water conditions were established using TDR sensor data collected from the field at the time of planting during the establishment year (2020).

Table 4: Soil physical and hydraulic properties by depth, including texture (clay and silt content), organic carbon, field capacity (FC), permanent wilting point (PWP), bulk density, soil root growth factor, and saturated water content in the experimental field. Source: USDA-NRCS Web Soil Survey (Soil Survey Staff, 2025).

Depth (cm)	Clay (%)	Silt (%)	Organic Carbon (%)	FC (cm³ cm⁻³)	PWP (cm³ cm⁻³)	Bulk Density (g/cm³)	Soil Root Growth Factor	Saturated water content (cm³ cm⁻³)
0-5	31	34	1.5	0.36	0.24	1.28	1	0.481
5-10	31	34	1.5	0.36	0.24	1.28	1	0.481
10-30	48	29	.8	0.36	0.24	1.3	1	0.478
30-50	48	29	0.8	0.43	0.32	1.3	0.449	0.478
50-70	48	29	0.8	0.43	0.32	1.3	0.301	0.478
70-80	48	29	0.8	0.43	0.32	1.3	0.223	0.478
80-100	48	29	0.8	0.43	0.32	1.3	0.165	0.478

3.3.3. Alfalfa Field Management

Field management data primarily include alfalfa cultivar details, planting method, planting date, seeding depth, planting density, irrigation treatments and timing, as well as fertilizer type, application rate, and timing. The experimental design was a strip-plot, with three irrigation treatment levels, two alfalfa cultivars, a drought-tolerant cultivar (Ladak II) with an FD of 2, and a highly productive cultivar (Stratica) with an FD of 4.3, both with a winter hardiness rating of 2. The three irrigation treatments were: i) Full Irrigation (FI), defined as full replenishment of soil water depletion to Field capacity (FC) in the top 1.5 m of soil; ii) mild Deficit Irrigation (DI), defined as the constant application of 80% of FI; and iii) moderate DI, defined as the constant

application of 60% of FI. Alfalfa was sown at 24 kg/ha (pure live seed) on 8 September 2020 in 9.14 m × 1.63 m plots. Phosphorus P₂O₅-67 kg/ha was uniformly applied, and plant height, LAI were periodically measured to assess plant growth. At the early flowering stage of alfalfa, an area of 5.57 m² inside each plot was harvested with a research plot harvester (36A, RCI Engineering, Mayville, WI), and the fresh biomass collected from each plot was weighed after harvest (EZ 400, Topcon Agriculture, Livermore, CA). A biomass subsample of approximately 500 g was collected from each plot to determine moisture, dry matter content, and nutritive value. The fresh subsample from each plot was dried at 66° C for 72 hours in a convection oven (Heratherm, Thermo Fisher Sc., Waltham, MS). Four cuts were made in each 2021, 2022, and 2023 growing seasons, with intervals between cuts of approximately 28 days (Table 5).

Table 5: Harvest Dates of Alfalfa During the 2021-2023 Growing Seasons.

Year	Date of harvest	Harvest Number
2021	15 June	First Harvest
	15 July	Second Harvest
	16 August	Third Harvest
	23 September	Fourth Harvest
2022	8 June	First Harvest
	8 July	Second Harvest
	4 August	Third Harvest
	31 August	Fourth Harvest
2023	8 June	First Harvest
	18 July	Second Harvest
	24 August	Third Harvest
	23 September	Fourth Harvest

All field management data was entered into DSSAT using the XBuild tool, ATCreate, and MOW input file formats. Within the XBuild experimental file, the Penman-Monteith FAO-56 method (Allen et al., 1998) was used to estimate Reference ET (ET_o), while the CENTURY soil organic matter model (Malik et al., 2018) was used to simulate carbon and nutrient cycling processes. After preparing all required input files, the CSM-CROPGRO-PFM was executed to assess its performance in simulating alfalfa growth and yield.

The initial simulations were performed using the default genotype parameters of the alfalfa cultivar ‘Oneida VR’, which has an FD rating of 3 (Jing et al., 2020). These parameters included

cultivar (genetic traits specific to an individual cultivar), ecotype (regional adaptation traits shared among related cultivars), and species (fundamental physiological traits of the crop) related parameters. The dormancy level of ‘Oneida VR’ was chosen as it represents an intermediate growth habit between the two cultivars used in this experiment, ‘Ladak II’, a drought-tolerant cultivar with low fall dormancy, and ‘Stratica’, a high-yielding cultivar with moderate fall dormancy. Using ‘Oneida VR’ as the starting reference allowed for baseline simulations of both cultivars before model calibration and parameter adjustments.

3.4. Model Sensitivity Analysis, Calibration, and Evaluation

After simulating alfalfa yield using the ‘Oneida VR’ cultivar, a sensitivity analysis was performed to identify the model parameters that most strongly influence simulated yield outcomes. The initial analysis was conducted using the DSSATSens utility tool available within DSSAT, which allows users to examine the model’s sensitivity to changes in input parameters while keeping all other variables constant. In its standard configuration, DSSATSens follows an OAT approach, where each parameter is systematically varied across a defined range while the others remain fixed (Jones et al., 2003). To enhance precision and automate the process, a Python-based OAT sensitivity analysis pipeline was developed. This automated script applied parameter perturbations (± 1 , ± 2 , ± 3 , ± 4 , ± 5 units) within the cultivar and the ecotype files. For each modified configuration, the DSSAT model was executed, and the resulting FORAGE.OUT file was parsed to extract simulated yield data. These simulated values were then merged with observed field data to compute statistical performance metrics. Finally, the percentage change in Root Mean Square

Error (RMSE) relative to the baseline was calculated to rank parameters based on their impact on model accuracy.

For the calibration stage, a Genetic Algorithm (GA) was implemented using PyGAD, an open-source Python library for evolutionary optimization (Gad, 2021), to optimize the most sensitive parameters identified through sensitivity analysis. PyGAD provides a flexible framework for automated parameter tuning by iteratively minimizing the difference between simulated and observed yields. In this study, GA was applied to search for optimal parameter combinations that minimized the differences between the observed and simulated alfalfa yields. The genetic parameters adjusted during calibration were limited to the cultivar (.CUL) and ecotype (.ECO) files, while the species (.SPE) file remained unchanged, as it contains fundamental physiological traits of the crop that are considered conservative and are not typically modified during regional calibration (Kothari et al., 2019).

The dataset was divided by growing season, with 2021 and 2022 data used for model calibration and 2023 data reserved for model evaluation. This approach ensured that the model's predictive capability was independently validated, confirming its accuracy and robustness across different years and irrigation treatments. A two-stage calibration approach was followed: first, a general calibration was performed with three irrigation treatments but using combined data from two cultivars to establish baseline parameter values. Then, cultivar-specific calibration was conducted to assess how two different cultivars, individually with the three irrigation treatments, influence model performance. This staged approach ensured that parameter optimization was cultivar-specific, enhancing the model's ability to represent field conditions realistically. During calibration, the GA iteratively adjusted key cultivar and ecotype parameters with the objective of

minimizing the RMSE between simulated and observed yields. The iterative optimization process followed by the GA is illustrated in Figure 5, showing how the population evolves through evaluation, reproduction, crossover, and mutation steps until the minimum RMSE criterion is achieved. The detailed steps involved in parameter calibration, including sensitivity analysis, optimization, and evaluation stages, are summarized in Figure 4, which presents the overall flowchart of the parameter calibration process.

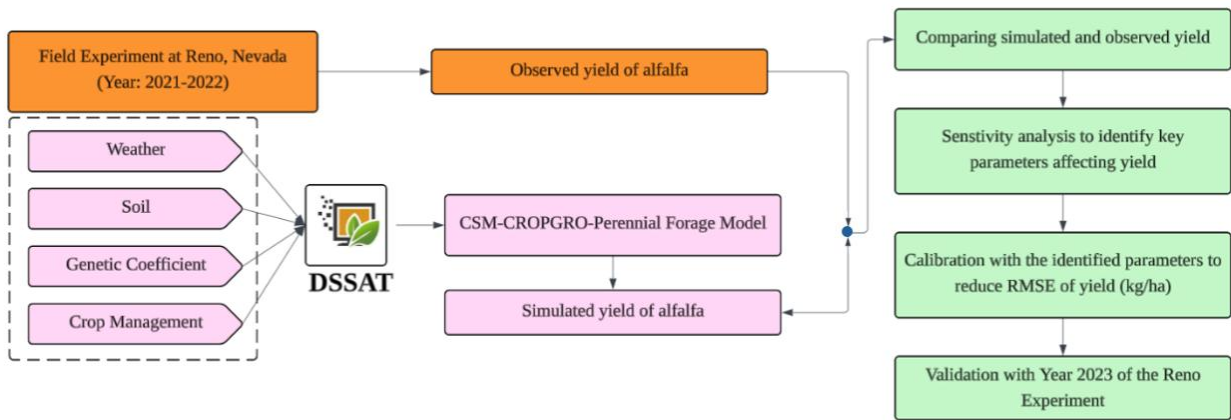


Figure 4: Workflow of model calibration and validation process for alfalfa yield simulation using the CSM-CROPGRO-PFM.

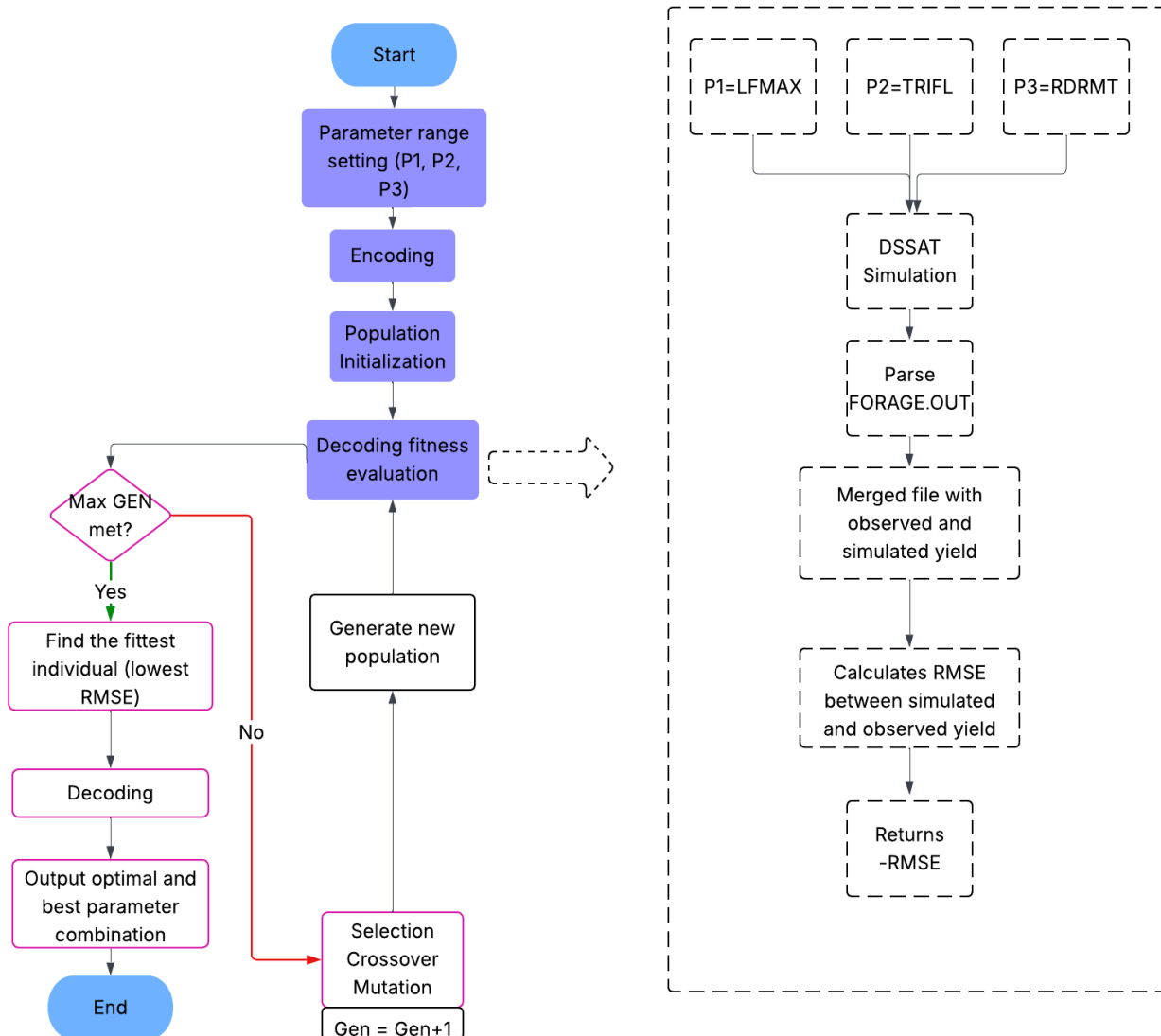


Figure 5: Workflow of the calibration process using a Genetic Algorithm integrated with DSSAT.

3.5. Performance Statistics

Model performance was evaluated using a combination of statistical performance indicators to assess the agreement between simulated and observed values (Adhikari et al., 2016; Beaudoin et al., 2008). The statistical indicators used included root mean square error (RMSE), normalized root mean square error (nRMSE), coefficient of determination (R^2), Nash-Sutcliffe model

efficiency (EF), and Willmott's index of agreement (d). The mathematical expressions for these indicators are given in Equations (1-5):

$$\text{Equation 1} \quad RMSE = \sqrt{\left(\frac{\sum(Y_i - X_i)^2}{n}\right)}$$

$$\text{Equation 2} \quad nRMSE = \frac{RMSE}{\bar{X}} \times 100$$

$$\text{Equation 3} \quad R^2 = \left(\frac{\sum(Y_i - \bar{Y})(X_i - \bar{X})}{\sqrt{\sum(Y_i - \bar{Y})^2} \sqrt{\sum(X_i - \bar{X})^2}} \right)^2$$

$$\text{Equation 4} \quad EF = 1 - \frac{\sum(Y_i - X_i)^2}{\sum(X_i - \bar{X})^2}$$

$$\text{Equation 5} \quad d = 1 - \frac{\sum(Y_i - X_i)^2}{\sum(|Y_i - \bar{X}| + |X_i - \bar{X}|)^2}$$

where Y_i and X_i represent the simulated and observed biomass values (i.e., alfalfa yield), respectively, \bar{Y} is the mean of simulated values, \bar{X} is the mean of observed values, and n is the number of observations.

Model performance was interpreted following established benchmarks (Bannayan & Hoogenboom, 2009). The model was considered excellent when $R^2 > 0.9$, EF , and $d \geq 0.9$, and $nRMSE \leq 10\%$; good when R^2 ranged between 0.8-0.9, EF between 0.75-0.9, and $nRMSE$ 10-20%; and fair to acceptable when $R^2 > 0.6$ and $nRMSE$ between 20-30%. Values of $EF \leq 0$ or $d < 0.6$ indicate poor predictive performance. The $RMSE$ values are expected to approach zero, denoting minimal bias and stronger agreement between simulated and observed data. Overall, model calibration and evaluation were considered satisfactory when $nRMSE$ is below 30%, $EF > 0.7$, and $d > 0.8$.

4. Results and Discussion

4.1. Sensitivity Analysis

The one-at-a-time (OAT) sensitivity analysis was conducted on 38 cultivar (.CUL) and ecotype file (.ECO) parameters to identify those exerting the greatest influence on simulated yield. Among these, TRIFL, LFMAX, and RDRMT emerged as the most sensitive parameters affecting yield variability (Table 6).

Table 6: Summary of sensitivity analysis for key cultivar and ecotype parameters.

Parameter	Baseline Value	Tested Range	Average RMSE (kg/ha)	% Change of RMSE from Baseline	Rank
TRIFL	0.22	± 0.05	1308	+ 78.3%	1
LFMAX	1.32	± 0.5	1244	+ 69.4%	2
RDRMT	0.500	± 0.5	978	+ 33.2%	3

- TRIFL, the rate of leaf appearance on the mainstem (leaves per thermal day) (Thorp et al., 2020; Jones et al., 2017) was the most influential parameter, producing an average RMSE of 1,308 kg/ha. Faster leaf appearance promotes canopy closure, increasing radiation interception and photosynthetic efficiency, thereby enhancing dry-matter accumulation. Conversely, slower leaf appearance delays canopy development and limits light interception (Teixeira et al., 2011).
- LFMAX, the maximum leaf photosynthetic rate ($\text{mg CO}_2 \text{ m}^{-2} \text{ s}^{-1}$), (Jones et al., 2017) ranked second in sensitivity, with an average RMSE of 1,244 kg/ha. Higher LFMAX values increased

the rate of daily carbon assimilation and biomass accumulation, highlighting that photosynthetic efficiency strongly governs yield potential.

- RDRMT, the relative dormancy sensitivity to daylength for partitioning (0-1 scale), ranked third, with an average RMSE of 978 kg/ha. High RDRMT values (strong dormancy) reduce above-ground growth and yield, whereas low values extend vegetative growth, increasing cumulative biomass (Malik et al., 2018; Raes et al., 2023).

These findings are consistent with prior CSM-CROPGRO-PFM studies for alfalfa (Boote et al., 2022; Malik et al., 2018), which identified LFMAX and RDRMT as critical parameters influencing yield predictions. The strong response of TRIFL might indicate the dominant role of canopy development and leaf regrowth after dormancy in controlling seasonal productivity in northern Nevada, where leaf regrowth after dormancy (i.e., during the first cutting period) results in the highest yield among all cutting periods (Cholula et al., 2024). These parameters were therefore selected for GA calibration.

4.2. Model Calibration and Validation

4.2.1. Stage 1: General Calibration

The first calibration stage optimized TRIFL, LFMAX, and RDRMT simultaneously across three irrigation treatments for the 2021-2022 growing season with the two cultivars combined. Relative to the initial DSSAT run using ‘Oneida VR’ default parameters, the GA produced small but consistent improvements and achieved convergence after several generations (Figure 7). For the calibration years 2021-2022, RMSE decreased from 748 to 723 kg/ha, nRMSE from 17.2 to 16.7%, R^2 increased slightly from 0.87 to 0.88 (Figure 6), and both EF and d improved to 0.88 and 0.97, respectively (Table 9). That means the model was already ‘good’ with the Oneida VR

cultivar, but the GA calibration resulted in a slight increase in accuracy. Also, the improvements occurred without overfitting the model to any specific irrigation level, showing that the three chosen parameters are indeed the dominant levers for this site.

Results obtained from this calibration stage, therefore, support the first hypothesis H1 (“The CSM-CROPGRO-PFM model, when calibrated with multi-year and multi-harvest field data from Northern Nevada, will simulate alfalfa growth and yield in the region across different cultivars and irrigation treatments with a satisfactory accuracy”) because the model reached what Bannayan & Hoogenboom (2009) call the ‘good’ zone ($R^2 \geq 0.8$, $nRMSE \approx 15-20\%$, $d \geq 0.9$) for the calibrated years.

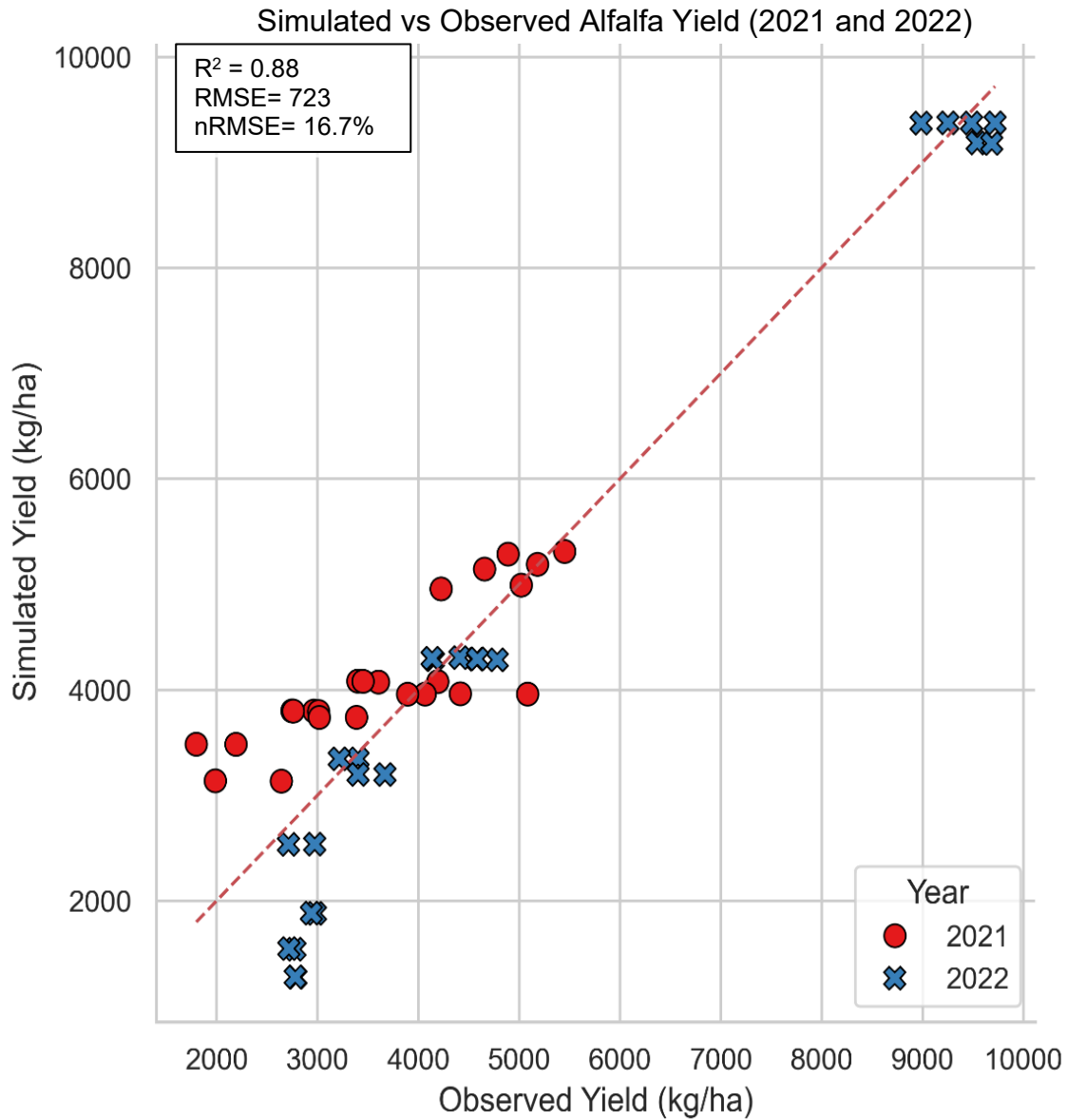


Figure 6: Simulated versus observed alfalfa yield for the 2021 and 2022 growing seasons under full and deficit irrigation treatments after the first stage of calibration. Each point (2021) or cross (2022) represents an individual cut across both cultivars (Ladak II and Stratica). The 1:1 dashed red line indicates perfect agreement between observed and simulated yields.

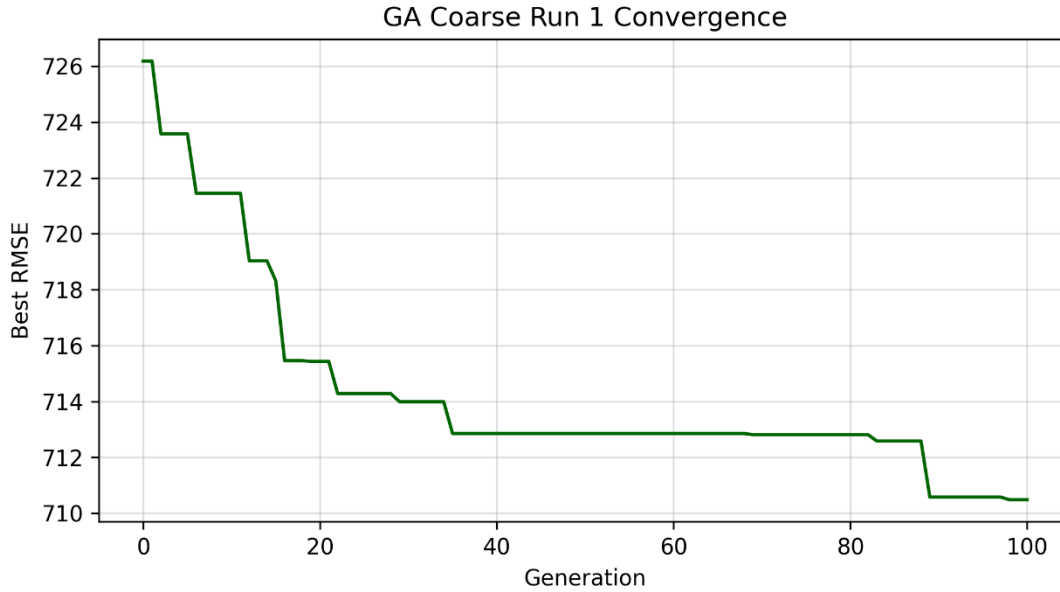


Figure 7: Convergence curve of Genetic Algorithm (GA) during the first calibration stage.

4.2.2 Stage 2: Cultivar-Specific Calibration

To capture genetic variability, cultivar-specific calibrations were performed for Ladak II and Stratica. The optimized parameters obtained with the GA (Table 7) reveal physiologically meaningful differences between cultivars.

Table 7: Comparison of parameter values before, in stage 1, and in stage 2 calibration.

Parameter	Starting Values (before calibration)	Calibrated Values (Stage 1: General calibration)	Calibrated Values (Stage 2: cultivar-specific calibration)	
			Ladak II	Stratica
TRIFL	0.22	0.20	0.25	0.23
LFMAX	1.32	1.21	1.20	1.23
RDRMT	0.500	0.294	0.247	0.396

Ladak II exhibited higher TRIFL and lower LFMAX and RDRMT, consistent with rapid canopy formation and reduced dormancy sensitivity, traits that contribute to drought tolerance and persistence under water stress (Orloff & Putnam, 2015). Stratica showed slightly higher LFMAX and RDRMT and lower TRIFL, reflecting stronger photoperiod responsiveness and a tendency for vegetative growth under favourable moisture conditions. An inversion was observed in RDRMT values between cultivars: Ladak II (more dormant) exhibited a lower RDRMT, while Stratica (less dormant) had a higher RDRMT. This likely resulted from parameter compensation during optimization. GA minimized RMSE by adjusting parameters beyond physiological expectations, a phenomenon also reported by Rabson et al. (2023). The cultivar-specific calibration slightly improved accuracy for 2021-2022 calibration years (RMSE = 715 kg/ha, nRMSE = 16.5%, EF = 0.88, $d = 0.97$) (Figure 8) (Table 9), which enhances biological realism while maintaining statistical performance.

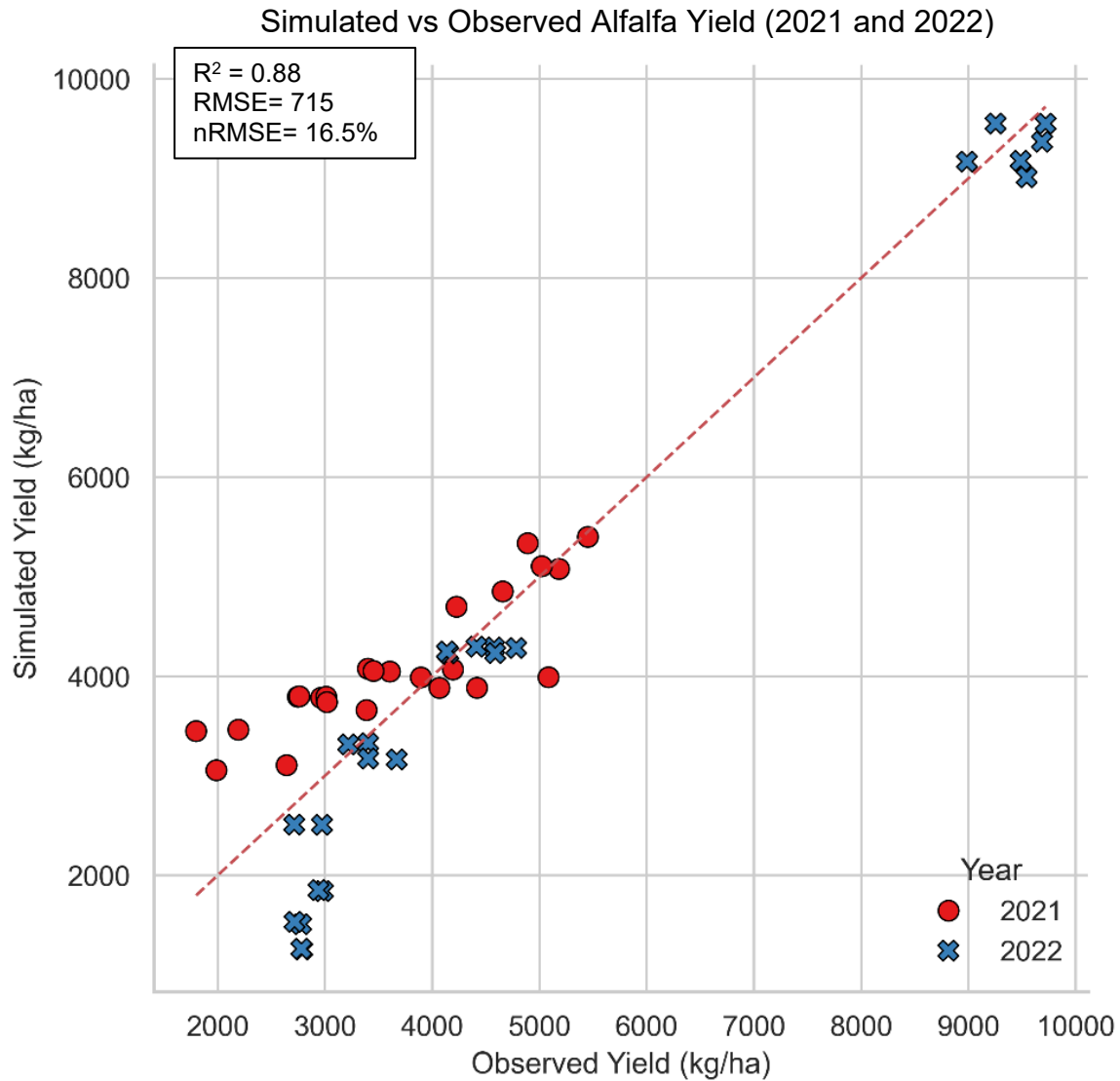


Figure 8: Simulated versus observed alfalfa yield for the 2021 and 2022 growing seasons after cultivar-specific GA calibration, showing improved alignment across irrigation treatments and cultivars with respect to the general calibration (Stage 1).

4.2.3 Evaluation Year - 2023

To assess model robustness and evaluate the newly optimized parameters after Stage 1 (general) and Stage 2 (cultivar-specific) calibration, alfalfa yield data collected during the 2023 growing season (excluded from the calibration process) were used for model evaluation. Model

accuracy declined modestly during this independent validation. For the default Oneida VR parameters in 2023, RMSE was 1,685 kg/ha, nRMSE = 39.3%, EF = 0.37, and d = 0.89. After the general calibration, RMSE improved slightly to 1,601 kg/ha (nRMSE = 37.3%), EF increased to 0.43, and d improved to 0.90 (Table 9). However, the cultivar-specific calibration increased RMSE to 1,695 kg/ha and reduced EF to 0.36, despite maintaining a high R^2 of 0.92 (Figure 9). These results indicate that the general calibration was more robust than the cultivar-specific parameterization when applied to the 2023 season. This reduced performance is likely due to several climatic and management conditions in 2023 that were not represented in the calibration dataset.

First, the 2023 season experienced unusually cold early-spring temperatures, with minimum spring temperatures dropping to $-8.6\text{ }^{\circ}\text{C}$ before the first harvest, much lower than the minimum spring temperatures in 2021 ($-2.5\text{ }^{\circ}\text{C}$) and 2022 ($-4.6\text{ }^{\circ}\text{C}$) (Figure 3). This indicates that 2023 experienced significantly colder early-season conditions and lower maximum and minimum temperatures. Thermal accumulation during spring was also considerably lower. According to Cholula Rivera (2025), only $16.15\text{ }^{\circ}\text{C}$ growing degree days were accumulated in March 2023, compared with $40.25\text{ }^{\circ}\text{C}$ in 2021 and $122.8\text{ }^{\circ}\text{C}$ in 2022. This lack of early-season heat delayed canopy development and suppressed first-cut biomass, which is typically the major contributor to total seasonal yield (Orloff & Putnam, 2015; Cholula et al., 2024). Because the cultivar-specific parameters were calibrated under warmer and more stable spring conditions, they overpredicted early-season growth when applied to the cooler 2023 environment.

Precipitation patterns also differed substantially. Cumulative rainfall in 2023 reached 276 mm, approximately 31% higher than in 2021 (211 mm) and 146% higher than in 2022 (112

mm) (Figure 3). This increased rainfall likely altered soil-moisture dynamics, contributing to discrepancies between expected and actual crop responses.

Irrigation management was another major deviation. Irrigation frequency declined sharply from 44 events in 2021 to 25 in 2022 and to only ~20 in 2023 for one treatment plot. Total seasonal irrigation volumes similarly decreased:

- **2021:** 1,589 mm (FI), 1,318 mm (mild DI), 1,043 mm (moderate DI)
- **2022:** 1,464 mm (FI), 1,280 mm (mild DI), 1,081 mm (moderate DI)
- **2023:** 1,021 mm (FI), 833 mm (mild DI), 632 mm (moderate DI)

The reduced irrigation demand in 2023 can be partly attributed to the substantially higher cumulative rainfall received that season, which limited the need for scheduled irrigations. In addition, thunderstorms in May and June of 2023 provided supplemental moisture, which is uncommon for this region during that period. These climatic anomalies likely contributed to both the lower number of irrigation events and the reduced seasonal irrigation totals observed in 2023. The resulting lower irrigation volumes and the longer intervals between applications in 2023 differed markedly from the conditions during the calibration period (2021–2022), when irrigation was more frequent and more consistent. Collectively, the combination of reduced spring thermal time, colder early-season temperatures, substantially higher rainfall, and lower irrigation frequency created environmental and water management conditions in 2023 that were markedly different than the conditions in the 2021-2022 calibration dataset. As a result, the cultivar-specific parameters tuned to warmer, more consistent growing conditions tended to overestimate early-season biomass and total yield during the evaluation year. The general calibration, being less specialized, was more robust to these typical conditions.

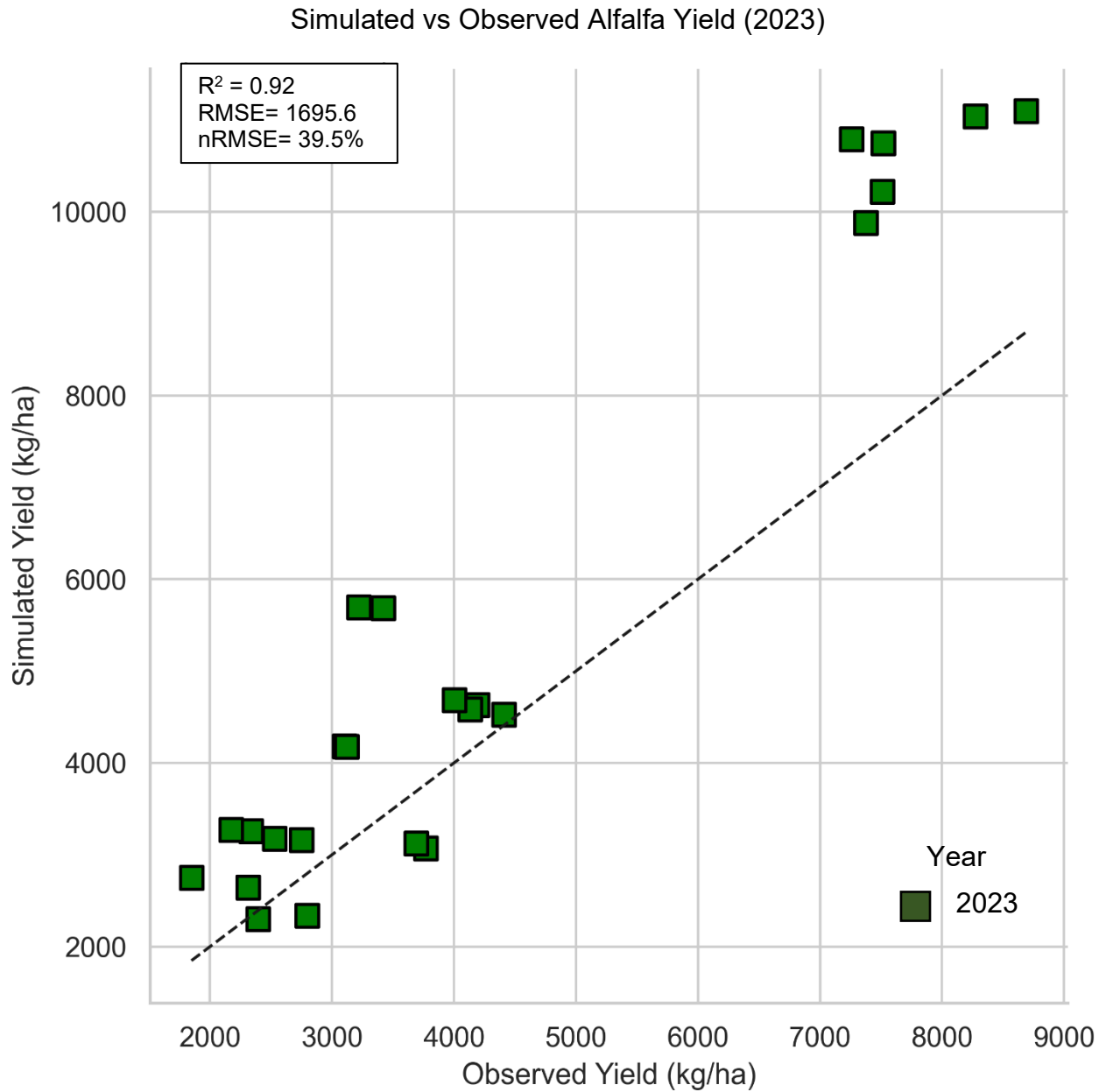


Figure 9: Simulated versus observed alfalfa yields for the 2023 evaluation year after 2 stages of GA calibration. Each point (2023) represents an individual cut across both cultivars (Ladak II and Stratica) and three irrigation treatments. The 1:1 dashed red line indicates perfect agreement between observed and simulated yields.

4.2.4 Treatment-Specific Model Performance

After two stages of calibration, model performance statistics for each cultivar and treatment combination are summarized in Table 8. Across treatments, R^2 ranged from 0.73 to 0.87, and $d > 0.90$, indicating strong agreement between the observed and simulated yield patterns. Despite the overall good fit, the model overestimated yields by 3-14% across all irrigation treatments and cultivars. This overprediction was more evident under mild deficit irrigation (80% FI) and for the Ladak II cultivar (Table 8).

The consistent overestimation following Stage 2 calibration suggests that the optimized parameters were tuned more closely to higher-yielding conditions, such as those observed under full irrigation, which dominated the calibration dataset. According to Cholula Rivera (2025), the mild deficit irrigation (80% FI) treatment frequently resulted in intermittent or delayed water stress, particularly for Ladak II, whose soil water depletion remained below the maximum allowable depletion threshold for a longer duration compared with Stratica in most years except for the mild DI in 2021. Because the Stage 2 calibration was primarily based on data from 2021-2022, when mild DI plots generally maintained near-optimal soil moisture, the optimization algorithm likely emphasized parameters (e.g., LFMAX, TRIFL, and RDRMT) that characterize well-watered or only slightly stressed conditions. As a result, the calibration dataset encompassed a relatively narrow range of environmental variability, limiting the model's ability to generalize to years or treatments with more pronounced or irregular water stress.

In 2023, when Ladak II experienced earlier and more persistent water stress, particularly after July (Cholula Rivera, 2025), the calibrated model tended to overpredict biomass accumulation. This occurred because the optimized parameter set implicitly assumed greater canopy development and radiation-use efficiency than what the actual field conditions supported. Consequently, the

systematic overestimation across treatments can be attributed to the dominance of non-stressed conditions in the training dataset and the model’s underrepresentation of water-stress effects on photosynthetic activity and growth. Additionally, residual uncertainty in the estimation of field capacity (FC) and permanent wilting point (PWP), even after model-based adjustments, may have contributed to inaccuracies in simulating soil-water balance and the timing of stress onset.

Table 8: Treatment-wise model performance for 2021, 2022, and 2023 growing seasons after stage 2 calibration.

Treatment	Mean		Ratio	r-Square	RMSE	d-Stat.	Total Number Obs.
	Observed	Simulated					
100% + Stratica	4587	4968	1.08	0.73	1336	0.90	12
80% + Stratica	4352	4789	1.09	0.83	1147	0.92	12
60%+ Stratica	4035	4160	1.02	0.85	1002	0.95	12
100% + Ladak II	4608	5066	1.10	0.84	1128	0.94	12
80% + Ladak II	4416	4903	1.11	0.87	1068	0.94	12
60%+ Ladak II	3882	4260	1.14	0.83	1129	0.94	12

Overall, simulated yield consistently declined with irrigation reduction (Figure 10), confirming CROPGRO-PFM’s ability to capture the direction and magnitude of yield responses to water limitation. However, the systematic overestimation suggests that further refinement of cultivar- and ecotype-specific parameters is needed to improve the model’s representation of partial water-stress conditions.

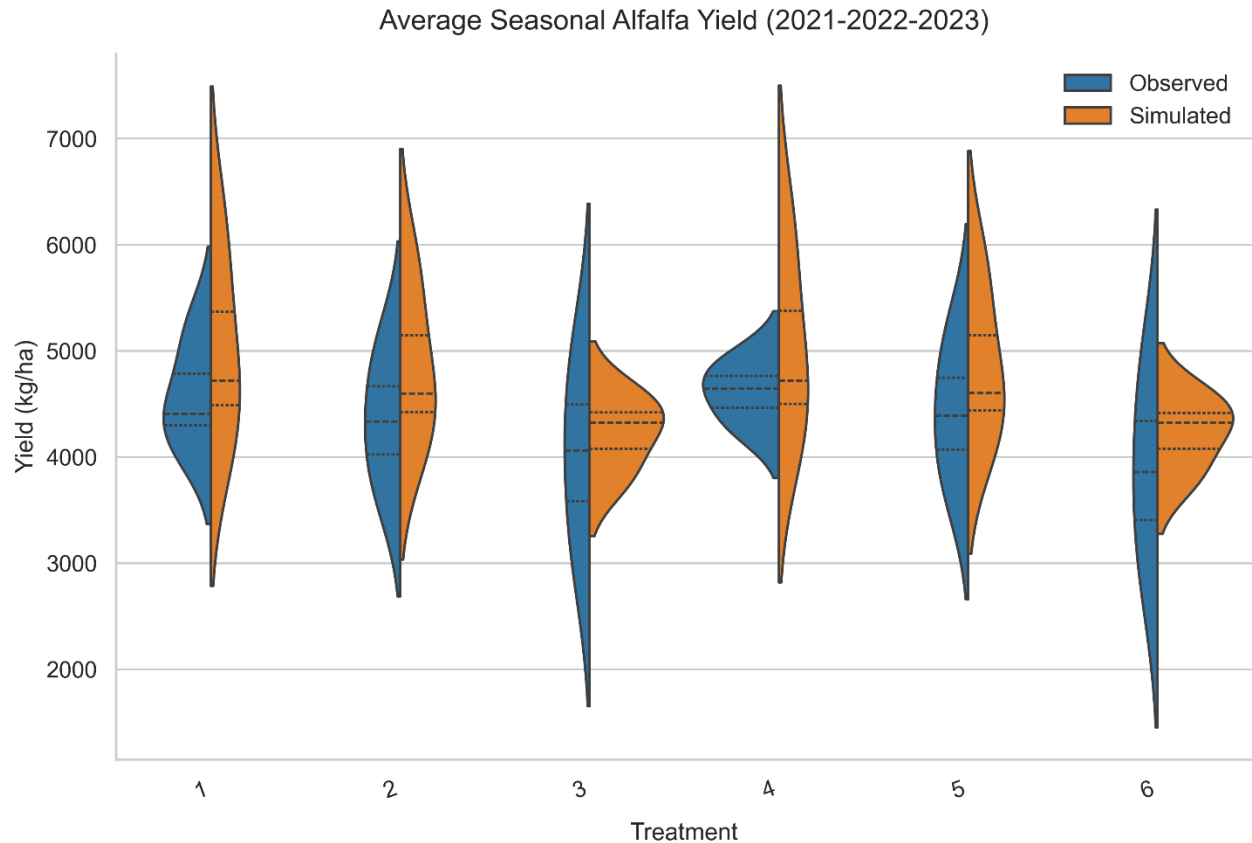


Figure 10: Comparison of overall average observed and simulated seasonal alfalfa yields across irrigation treatments (100 %, 80 %, and 60 % FI) and cultivars (Ladak II and Stratica) during 2021-2023. Where 1 is 100% + Stratica, 2 is 80% + Stratica, 3 is 60% + Stratica, 4 is 100% + Ladak II, 5 is 80% + Ladak II, and 6 is 60% + Ladak II.

4.2.5 Cut-Wise Yield Patterns

Following treatment-level validation, the model’s growing season was examined using cut-wise yields (Figure 11). The model accurately reproduced the seasonal trend characterized by the first cut (C1) producing the highest yield, followed by a progressive decline in subsequent cuts (C2 - C4) due to increased evapotranspiration and reduced regrowth potential during mid-summer (Cholula Rivera, 2025).

Across all three years, the simulated trends closely matched the observed data, demonstrating the model’s ability to capture regrowth and harvest timing effects under variable environmental

conditions. The first-cut peak values were well aligned between observed and simulated values, particularly in 2021 and 2022, when early-season moisture and favourable spring temperatures (Figure 3) supported faster biomass accumulation compared to 2023. Major deviations occurred during C2 and C3, especially in 2023, where the model slightly overestimated mid-season yields. This is likely reflecting an underestimation of cumulative water stress and soil moisture depletion following early high production.

Overall, Figures 10 and 11 illustrate how the calibrated CROPGRO-PFM successfully simulates the multi-harvest growth dynamics of alfalfa across years and irrigation regimes. The consistent alignment between observed and simulated data supports hypothesis H2 (“The model will capture key agronomic patterns, such as higher yields in the first harvest and decreasing yields in subsequent cuts, as well as yield reductions under increasing water stress”), confirming that the model can effectively capture yield variability among cuts and respond accurately to water stress-induced yield reduction patterns.

Cut-wise Observed vs Simulated Alfalfa Yield (2021-2022-2023)

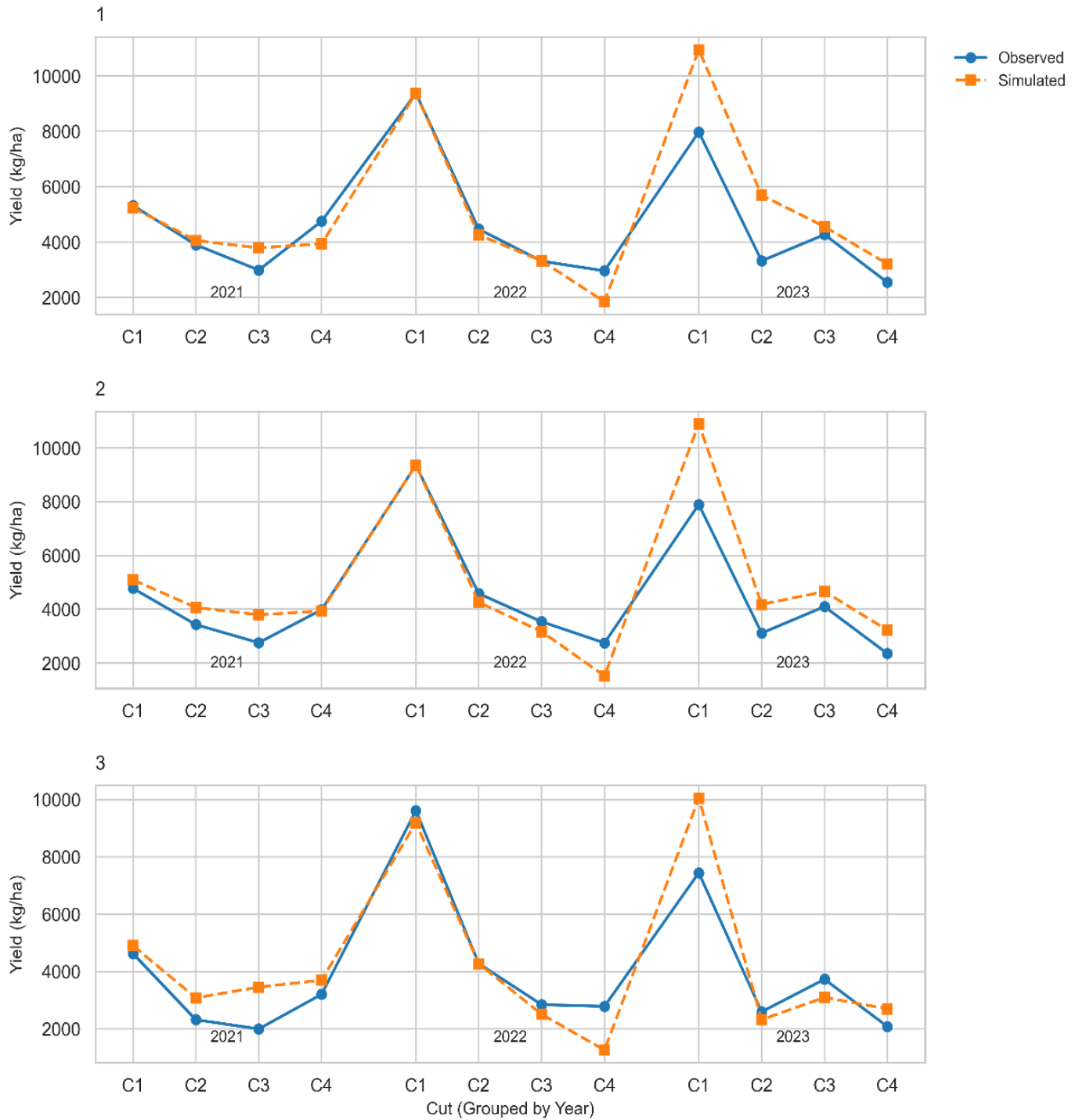


Figure 11: Observed and simulated cut-wise yields under 1=100 %, 2=80 %, and 3=60 % irrigation treatments for years 2021, 2022, and 2023 across both cultivars after 2 stages of GA calibration. Here, C1 is the first cut, C2 is the second cut, C3 is the third cut, and C4 is the fourth cut.

4.2.6 Overall Performance

When all three years were pooled, the GA Stage 1 calibration reduced the overall RMSE from 1149 to 1097 kg/ha and nRMSE from 26.6 to 25.4 %. R^2 improved from 0.82 to 0.83 and EF from 0.7 to 0.73, with d remaining high from 0.93 to 0.94 (Figure 12) (Table 9). After Stage 2, RMSE slightly increased (1140 kg/ha), confirming that cultivar-specific calibration provides greater biological clarity but does not necessarily yield a better three-year overall performance.

This decline in overall accuracy after Stage 2 may be partly attributed to the reduced sample size available for calibration. Because Stage 2 divides the dataset by cultivar, each model simulation is trained on roughly half the data used in Stage 1. This partitioning limits the range of environmental and management conditions on which the optimization algorithm is trained, thereby slightly reducing its ability to generalize across all years. Despite this, the cultivar-specific calibration remains important for distinguishing physiological and phenological differences among cultivars.

Even so, $EF \geq 0.70$ and $d \geq 0.94$ (Table 9) are considered satisfactory for a perennial, multi-harvest, deficit-irrigated system. Therefore, hypothesis H3 (“Calibrating the most sensitive parameters with the genetic algorithm will significantly improve the model’s performance metrics”) was met for the calibration years and partially met for the evaluation year.

Simulated vs Observed Alfalfa Yield (2021, 2022, and 2023)

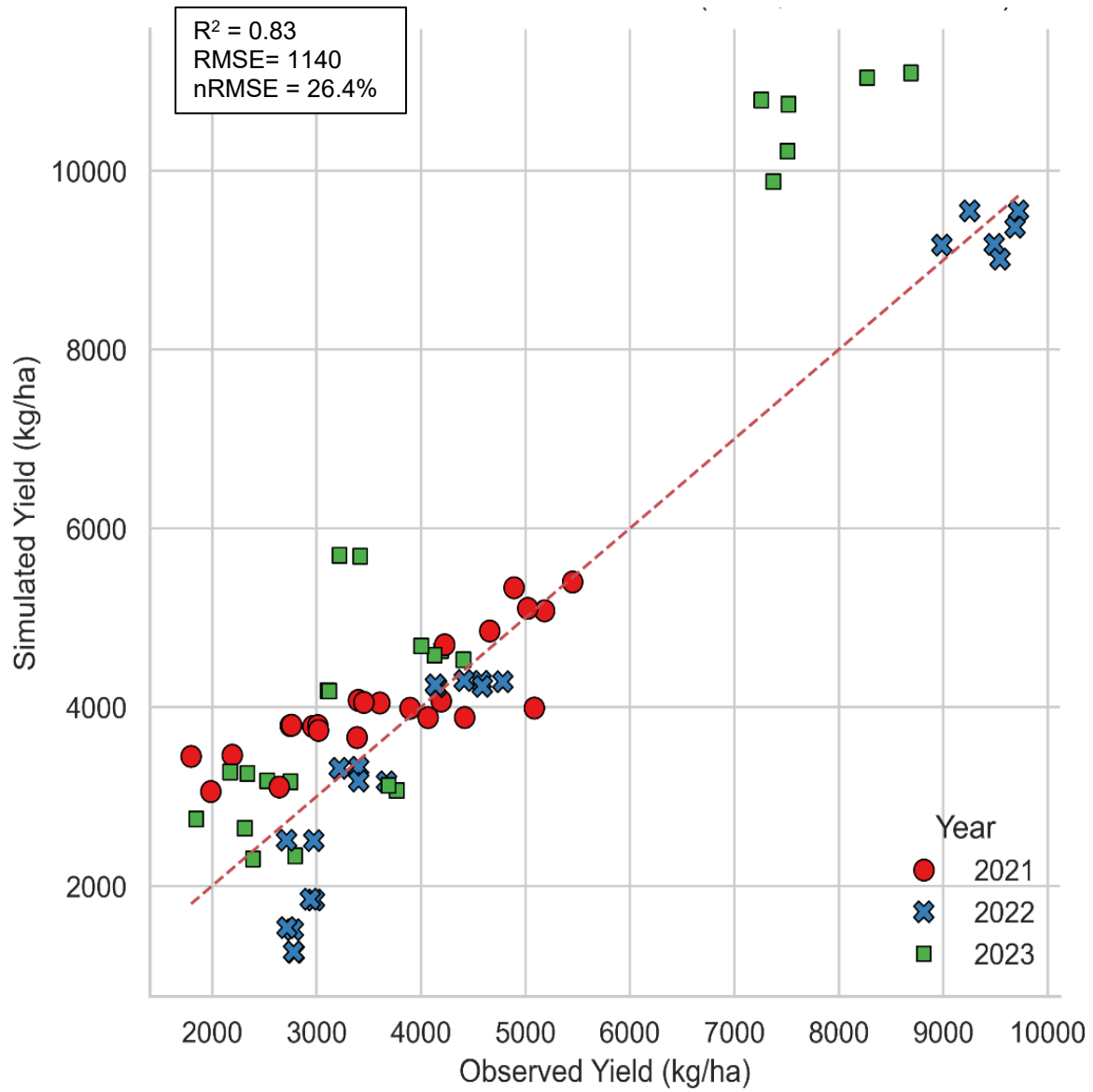


Figure 12: Simulated versus observed yields for the years 2021, 2022, and 2023 after 2 stages of GA calibration. The 1:1 dashed red line indicates perfect agreement between observed and simulated yields.

Table 9: Comparison of model performance across calibration stages and years.

Years	Average Statistics across treatments and cultivars	Initial Simulation Results with 'Oneida VR' Cultivar	Stage 1: General Calibration Results	Stage 2: Specific Calibration Results
2021+2022 (Calibration Years)	RMSE (kg/ha)	748	723	715
	nRMSE (%)	17.2	16.7	16.5
	R ²	0.87	0.88	0.88
	EF	0.875	0.88	0.88
	d	0.96	0.97	0.97
2023 (Evaluation Year)	RMSE (kg/ha)	1685	1601	1695
	nRMSE (%)	39.3	37.3	39.5
	R ²	0.91	0.92	0.92
	EF	0.37	0.43	0.36
	d	0.89	0.90	0.90
2021+2022+2023 (Overall Results)	RMSE (kg/ha)	1149	1097	1140
	nRMSE (%)	26.6	25.4	26.4
	R ²	0.82	0.83	0.83
	EF	0.70	0.73	0.71
	d	0.93	0.94	0.94

The results of this study align closely with trends reported in previous process-based alfalfa modeling efforts summarized in the literature review (Table 1). Similar to studies conducted in Spain, China, and Australia using CSM-CROPGRO-PFM, APSIM-Lucerne, and AquaCrop, the calibrated model in this study achieved a strong accuracy ($r^2 \geq 0.80$, nRMSE \approx 20-30%, $d \geq 0.9$) (Table 9), indicating its robustness in simulating alfalfa yield across varying irrigation levels and cultivars. However, unlike most published studies conducted under humid or semi-humid conditions, this work extends the application of CROPGRO-PFM to the arid western U.S., where water limitations and harsh, highly variable environmental conditions present unique modeling challenges. By demonstrating reliable performance under deficit irrigation and multi-harvest conditions, the present study advances the regional applicability of CSM-CROPGRO-PFM for alfalfa and provides new insights into parameter behavior in semi-arid, water-constrained systems.

5 Limitations of the Study

1. The OAT sensitivity analysis method did not account for potential interactions among the parameters.
2. Calibration relied solely on yield-based RMSE as the optimization criterion and excluded other physiological variables (e.g., LAI, biomass partitioning, soil moisture).
3. Model calibration and validation were based on a single experimental site and a single external evaluation year (2023), limiting the generalizability of the results across diverse soil types, climatic conditions, and management practices.
4. The weather and soil datasets were compiled from secondary sources (WRCC and NRCS), which may contain measurement errors or represent averaged conditions that do not fully capture within-field microclimate variability.

5. The soil hydraulic properties were adjusted empirically to match observed soil moisture trends.
6. Forage quality was not simulated, which might be a limiting application for nutritional assessments.
7. The stochastic nature of GA uses random initial populations and operators (mutation, crossover), so even with identical settings, the exact optimized parameter values differ between runs, which might potentially affect the reproducibility of this research.

6 Future Work

1. Conduct multi-site, multi-year validation to assess parameter transferability across different soil and climatic conditions.
2. Integrate soil moisture dynamics and other physiological variables into the calibration process to enhance model accuracy under deficit irrigation.
3. Expand the GA calibration to a multi-objective framework that simultaneously minimizes dry yield, LAI, plant height, and biomass estimation errors.
4. Incorporate forage quality parameters (e.g., crude protein) to include a nutritional perspective in model evaluation.
5. Integrate the fully developed model into the YFT for practical application across the western United States.

7 Conclusions

This study successfully calibrated and evaluated the CSM-CROPGRO-PFM to simulate alfalfa yield responses under full and deficit irrigation conditions in northern Nevada. Using three years of multi-harvest field data, the model effectively captured cultivar-specific and irrigation-level

variations in yield. The OAT sensitivity analysis identified TRIFL, LFMAX, and RDRMT as the most influential parameters affecting yield variability. Genetic Algorithm (GA) based calibration substantially improved model performance, reducing RMSE and nRMSE while increasing R^2 , EF, and Willmott's d statistics across the calibration years (2021-2022). Although accuracy declined during the 2023 evaluation year, likely due to environmental and management variability, the model maintained robust predictive ability ($R^2 > 0.9$). The generalized calibration proved more stable across years than cultivar-specific calibration, emphasizing the tradeoff between parameter specificity and transferability.

Overall, the calibrated CSM-CROPGRO-PFM demonstrated high reliability in simulating yield dynamics across irrigation regimes and harvests, validating its suitability for deficit irrigation management. These findings establish a strong foundation for developing an open-source Alfalfa Yield Forecasting Tool (YFT) designed to optimize irrigation scheduling, conserve water, and sustain forage productivity under limited water availability in arid and semi-arid regions.

References

- Adhikari, P., Gowda, P. H., Marek, G. W., Brauer, D. K., Kisekka, I., Northup, B., & Rocateli, A. (2017). Calibration and validation of CSM-CROPGRO-Cotton model using lysimeter data in the Texas High Plains. *Journal of Contemporary Water Research & Education*, 162(1), 61–78. <https://doi.org/10.1111/j.1936-704X.2017.03255.x>
- AkhavanZadegan, F., Ansarifar, J., Wang, L., Huber, I., & Archontoulis, S. V. (2021). A time-dependent parameter estimation framework for crop modeling. *Scientific Reports*, 11, 11437. <https://doi.org/10.1038/s41598-021-90984-4>
- Allen, R. G., Pereira, L. S., Raes, D., & Smith, M. (1998). *Crop evapotranspiration: Guidelines for computing crop water requirements (FAO Irrigation and Drainage Paper No. 56)*. Food and Agriculture Organization of the United Nations. <https://www.fao.org/3/x0490e/x0490e00.htm>
- Attia, A., El-Hendawy, S., Al-Suhaibani, N., Tahir, M. U., Mubushar, M., dos Santos Vianna, M., Ullah, H., Mansour, E., & Datta, A. (2021). Sensitivity of the DSSAT model in simulating maize yield and soil carbon dynamics in arid Mediterranean climate: Effect of soil, genotype, and crop management. *Field Crops Research*, 260, 107981. <https://doi.org/10.1016/j.fcr.2020.107981>
- Bai, Y., & Gao, J. (2021). Optimization of the nitrogen fertilizer schedule of maize under drip irrigation in Jilin, China, based on DSSAT and GA. *Agricultural Water Management*, 244, 106555. <https://doi.org/10.1016/j.agwat.2020.106555>
- Bai, Y., Yue, W., & Ding, C. (2022). Optimize the irrigation and fertilizer schedules by combining DSSAT and genetic algorithm. *Environmental Science and Pollution Research*, 29(39), 52473–52482. <https://doi.org/10.1007/s11356-022-19718-1>
- Beaudoin, N., Launay, M., Sauboua, E., Ponsardin, G., & Mary, B. (2008). Evaluation of the soil crop model STICS over 8 years against the “on farm” database of Bruyères catchment. *European Journal of Agronomy*, 29(1), 46–57. <https://doi.org/10.1016/j.eja.2008.03.001>
- Boote, K. J., Jones, J. W., & Hoogenboom, G. (2018). Simulation of crop growth: CROPGRO model. In *Agricultural systems modeling and simulation* (pp. 1–22). CRC Press. <https://doi.org/10.1201/9781482269765-18>
- Boote, K. J., Ottman, M., Torrion, J., Kisekka, I., Hoogenboom, G., & Malik, W. (2022, November). *Simulating alfalfa growth dynamics of fall dormancy classes across environments*. Proceedings of the Western California Alfalfa & Forage Symposium. University of California Cooperative Extension. <https://calhaysymposium.com/wp-content/uploads/2022/11/SIMULATING-ALFALFA-GROWTH-DYNAMICS-OF-FALL-DORMANCY-CLASSES-ACROSS-ENVIRONMENTS-Ken-Boote.pdf>
- Bourgeois, G. (1990). Evaluation of an alfalfa growth simulation model under Quebec conditions. *Agricultural Systems*, 32(1), 1–12. [https://doi.org/10.1016/0308-521X\(90\)90026-M](https://doi.org/10.1016/0308-521X(90)90026-M)
- Brisson, N., Mary, B., Ripoche, D., Jeuffroy, M. H., Ruget, F., Nicoullaud, B., Gate, P., Devienne-Barret, F., Antonioletti, R., Durr, C., Richard, G., Beaudoin, N., Recous, S., Tayot, X., Plenet, D., Cellier, P., Machet, J. M., Meynard, J. M., & Delécolle, R. (1998). STICS: A generic model for the simulation of crops and their water and nitrogen balances. I. Theory and

parameterization applied to wheat and corn. *Agronomie*, 18(5–6), 311–346. <https://doi.org/10.1051/agro:19980501>

Carter, C., Garcia y Garcia, A., Islam, M. A., & Hansen, K. (2013). Effect of deficit irrigation on water use and water use efficiency of alfalfa. *ASABE Annual International Meeting*, 1–12. <https://doi.org/10.13031/aim.20131603513>

Chapagain, R., Remenyi, T. A., Harris, R. M. B., Mohammed, C. L., Huth, N., Wallach, D., Rezaei, E. E., & Ojeda, J. J. (2022). Decomposing crop model uncertainty: A systematic review. *Field Crops Research*, 279, 108448. <https://doi.org/10.1016/j.fcr.2022.108448>

Cholula, U., Andrade, M. A., & Solomon, J. K. Q. (2024). Leaf area index estimation of fully and deficit irrigated alfalfa through canopy cover and canopy height. *AgriEngineering*, 6(3), 2101–2114. <https://doi.org/10.3390/agriengineering6030123>

Cholula, U., Quintero, D., Andrade, M. A., & Solomon, J. (2022). Effects of deficit irrigation on yield and water productivity of alfalfa in Northern Nevada. *2022 ASABE Annual International Meeting*. <https://doi.org/10.13031/aim.202201104>

Cholula Rivera, U. (2025). *Assessing the effects of deficit irrigation on alfalfa grown in Northern Nevada* (Doctoral dissertation). University of Nevada, Reno.

Colpan, C. O., Kizilkan, Ö., & Ezan, M. M. (2021). Multiobjective optimization of a geothermal power plant. In C. O. Colpan, Ö. Kizilkan, & M. M. Ezan (Eds.), *Thermodynamic analysis and optimization of geothermal power plants* (pp. 1–11). Elsevier. <https://doi.org/10.1016/C2020-0-02062-1>

Confalonieri, R., & Bechini, L. (2004). A preliminary evaluation of the simulation model CropSyst for alfalfa. *European Journal of Agronomy*, 21(2), 223–237. <https://doi.org/10.1016/j.eja.2003.08.003>

Denison, R. F., & Loomis, R. S. (1989). *An integrative physiological model of alfalfa growth and development* (Publication No. 1926). University of California, Division of Agriculture and Natural Resources.

Fereres, E., & Soriano, M. A. (2007). Deficit irrigation for reducing agricultural water use. *Journal of Experimental Botany*, 58(2), 147–159. <https://doi.org/10.1093/jxb/erl165>

Fick, G. W. (1981). *ALSIM 1 (Level 2) user's manual* (Mimeo. 81-35). Cornell University, Department of Agronomy.

Fink, K. P., Grassini, P., Rocateli, A., Bastos, L. M., Kastens, J., Ryan, L. P., Lin, X., Patrignani, A., & Lollato, R. P. (2022). Alfalfa water productivity and yield gaps in the U.S. central Great Plains. *Field Crops Research*, 289, 108728. <https://doi.org/10.1016/j.fcr.2022.108728>

Gad, A. F. (2020). *PyGAD: Python Genetic Algorithm library* (Version 3.5.0) [Computer software]. PyPI. <https://pygad.readthedocs.io/>

Gad, A. F. (2021). PyGAD: An intuitive genetic algorithm Python library. *arXiv*. <https://doi.org/10.48550/arXiv.2106.06158>

Holland, J. H. (1975). *Adaptation in natural and artificial systems*. University of Michigan Press.

Holt, D. A., Bula, R. J., Miles, G. E., Schreiber, M. M., & Peart, R. M. (1975). *Environmental physiology, modeling, and simulation of alfalfa growth: I. Conceptual development of SIMED (Bulletin No. 907)*. Purdue University.

Hoogenboom, G., Porter, C. H., Boote, K. J., Shelia, V., Wilkens, P. W., Singh, U., White, J. W., Asseng, S., Lizaso, J. I., Moreno, L. P., Pavan, W., Ogoshi, R., Hunt, L. A., Tsuji, G. Y., & Jones, J. W. (2019). The DSSAT crop modeling ecosystem. In K. J. Boote (Ed.), *Advances in crop modeling for a sustainable agriculture* (pp. 173–216). Burleigh Dodds Science Publishing. <https://doi.org/10.19103/AS.2019.0061.10>

Hoogenboom, G., Porter, C. H., Shelia, V., Boote, K. J., Singh, U., Pavan, W., Oliveira, F. A. A., Moreno-Cadena, L. P., Ferreira, T. B., White, J. W., Lizaso, J. I., Pequeno, D. N. L., Kimball, B. A., Alderman, P. D., Thorp, K. R., Cuadra, S. V., Vianna, M. S., Villalobos, F. J., Batchelor, W. D., Koo, J., Hunt, L. A., & Jones, J. W. (2024). *Decision Support System for Agrotechnology Transfer (DSSAT) Version 4.8.5*. DSSAT Foundation. <https://www.dssat.net>

Jégo, G., Rotz, C. A., Bélanger, G., Tremblay, G. F., Charbonneau, É., & Pellerin, D. (2015). Simulating forage crop production in a northern climate with the Integrated Farm System Model. *Canadian Journal of Plant Science*, 95(4), 745–757. <https://doi.org/10.4141/cjps-2014-375>

Jing, Q., Qian, B., Bélanger, G., VanderZaag, A., Jégo, G., Smith, W., Grant, B., Shang, J., Liu, J., He, W., Boote, K., & Hoogenboom, G. (2020). Simulating alfalfa regrowth and biomass in eastern Canada using the CSM-CROPGRO-Perennial Forage model. *European Journal of Agronomy*, 113, 125971. <https://doi.org/10.1016/j.eja.2019.125971>

Jones, J. W., Antle, J. M., Basso, B., Boote, K. J., Conant, R. T., Foster, I., Godfray, H. C. J., Herrero, M., Howitt, R. E., Janssen, S., Keating, B. A., Muñoz-Carpena, R., Porter, C. H., Rosenzweig, C., & Wheeler, T. R. (2017). Toward a new generation of agricultural system data, models, and knowledge products: State of agricultural systems science. *Agricultural Systems*, 155, 269–288. <https://doi.org/10.1016/j.agsy.2016.09.021>

Jones, J. W., Hoogenboom, G., Porter, C. H., Boote, K. J., Batchelor, W. D., Hunt, L. A., Wilkens, P. W., Singh, U., Gijsman, A. J., & Ritchie, J. T. (2003). The DSSAT cropping system model. *European Journal of Agronomy*, 18(3–4), 235–265. [https://doi.org/10.1016/S1161-0301\(02\)00107-7](https://doi.org/10.1016/S1161-0301(02)00107-7)

Karam, F., Saliba, R., Skaf, S., Breidy, J., Roupheal, Y., & Balendonck, J. (2011). Yield and water use of eggplants (*Solanum melongena* L.) under full and deficit irrigation regimes. *Agricultural Water Management*, 98(8), 1307–1316. <https://doi.org/10.1016/j.agwat.2011.03.012>

Keating, B. A., Carberry, P. S., Hammer, G. L., Probert, M. E., Robertson, M. J., Holzworth, D. P., Huth, N. I., Hargreaves, J. N. G., Meinke, H., Hochman, Z., McLean, G., Verburg, K., Snow, V., Dimes, J. P., Silburn, M., Wang, E., Brown, S., Bristow, K. L., Asseng, S., ... Smith, C. J. (2003). An overview of APSIM, a model designed for farming systems simulation. *European Journal of Agronomy*, 18(3–4), 267–288. [https://doi.org/10.1016/S1161-0301\(02\)00108-9](https://doi.org/10.1016/S1161-0301(02)00108-9)

Khanmohammadi, S., Kizilkan, Ö., & Musharavati, F. (2021). Multiobjective optimization of a geothermal power plant. In *Thermodynamic analysis and optimization of geothermal power plants* (pp. 279–291). Elsevier. <https://doi.org/10.1016/B978-0-12-821037-6.00011-1>

Kothari, K. (2019). *Assessing climate change adaptation strategies for major crops in Texas: A case study in two regions* (Doctoral dissertation). Texas A&M University. <https://oaktrust.library.tamu.edu/handle/1969.1/187508>

Lamb, J. F. S., Sheaffer, C. C., Rhodes, L. H., Sulc, R. M., Undersander, D. J., & Brummer, E. C. (2006). Five decades of alfalfa cultivar improvement: Impact on forage yield, persistence, and nutritive value. *Crop Science*, *46*(2), 902–909. <https://doi.org/10.2135/cropsci2005.0082>

Lamsal, A., Welch, S. M., Jones, J. W., Boote, K. J., Asebedo, A., Crain, J., Wang, X., Boyer, W., Giri, A., Frink, E., Xu, X., Gundy, G., Ou, J., & Arachchige, P. G. (2017). Efficient crop model parameter estimation and site characterization using large breeding trial data sets. *Agricultural Systems*, *157*, 170–184. <https://doi.org/10.1016/j.agsy.2017.07.016>

Li, J., Wang, R., Zhang, M., Wang, X., Yan, Y., & Xu, D. (2023). A method for estimating alfalfa (*Medicago sativa* L.) forage yield based on remote sensing data. *Agronomy*, *13*(10), 2597. <https://doi.org/10.3390/agronomy13102597>

Lindenmayer, R. B., Hansen, N. C., Brummer, J., & Pritchett, J. G. (2011). Deficit irrigation of alfalfa for water-saving in the Great Plains and Intermountain West: A review and analysis of the literature. *Agronomy Journal*, *103*(1), 45–50. <https://doi.org/10.2134/agronj2010.0204>

Ly, M., Tian, D., Wang, G., Fan, T., Li, W., Hou, C., Zhou, J., & Miao, X. (2025). Selection of alfalfa water and nitrogen management regimes based on the DSSAT model. *Scientific Reports*, *15*(1), 12108. <https://doi.org/10.1038/s41598-025-92058-w>

Ma, Q., Xu, X., Wang, W., Zhao, L., Ma, D., & Xie, Y. (2021). Comparative analysis of alfalfa (*Medicago sativa* L.) seedling transcriptomes reveals genotype-specific drought tolerance mechanisms. *Plant Physiology and Biochemistry*, *166*, 203–214. <https://doi.org/10.1016/j.plaphy.2021.05.008>

Malik, W., Boote, K. J., Hoogenboom, G., Cavero, J., & Dechmi, F. (2018). Adapting the CROPGRO model to simulate alfalfa growth and yield. *Agronomy Journal*, *110*(5), 1777–1790. <https://doi.org/10.2134/agronj2017.12.0680>

Malik, W., & Dechmi, F. (2019). DSSAT modelling for best irrigation management practices assessment under Mediterranean conditions. *Agricultural Water Management*, *216*, 27–43. <https://doi.org/10.1016/j.agwat.2019.01.017>

Miao, X., Wang, G., Li, R., Xu, B., Zheng, H., Tian, D., Wang, J., Ren, J., Li, Z., & Zhou, J. (2024). Study on modeling and evaluating alfalfa yield and optimal water use efficiency in the agro-pastoral ecotone of Northern China. *Plants*, *13*(2), 229. <https://doi.org/10.3390/plants13020229>

Miao, X., Wang, G., Xu, B., Li, R., Tian, D., Ren, J., Li, Z., Fan, T., Zhang, Z., & Xu, Q. (2025). Study on alfalfa water use efficiency and optimal irrigation strategy in agro-pastoral ecotone, Northwestern China. *Agronomy*, *15*(2), 258. <https://doi.org/10.3390/agronomy15020258>

Mitchell, M. (1996). *An introduction to genetic algorithms*. MIT Press. <https://doi.org/10.7551/mitpress/3927.001.0001>

Moot, D. J., Hargreaves, J., Brown, H. E., & Teixeira, E. I. (2015). Calibration of the APSIM-Alfalfa model for ‘Grasslands Kaituna’ alfalfa crops grown in New Zealand. *New Zealand Journal of Agricultural Research*, *58*(2), 190–202. <https://doi.org/10.1080/00288233.2015.1014362>

Mullins, C. R., Grigsby, K. N., & Bradford, B. J. (2009). Effects of alfalfa hay inclusion rate on productivity of lactating dairy cattle fed wet corn gluten feed-based diets. *Journal of Dairy Science*, 92(7), 3510–3516. <https://doi.org/10.3168/jds.2008-1873>

Nevada Annual Bulletin. (2025). *2023 Nevada agricultural statistics*. U.S. Department of Agriculture, National Agricultural Statistics Service. https://data.nass.usda.gov/Statistics_by_State/Nevada/Publications/Annual_Statistical_Bulletin/2020s/2023%20NV%20Annual%20Bulletin.pdf

Orloff, S., & Putnam, D. (2015). *Drought strategies for alfalfa (ANR Publication 8522)*. University of California Agriculture and Natural Resources. <https://anrcatalog.ucanr.edu>

Ojeda, J. J., Pembleton, K. G., Islam, M. R., Agnusdei, M. G., & Garcia, S. C. (2016). Evaluation of the Agricultural Production Systems Simulator simulating lucerne and annual ryegrass dry matter yield in the Argentine Pampas and south-eastern Australia. *Agricultural Systems*, 143, 61–75. <https://doi.org/10.1016/j.agsy.2015.12.005>

Pabico, J. P., Hoogenboom, G., & McClendon, R. W. (1999). Determination of cultivar coefficients of crop models using a genetic algorithm: A conceptual framework. *Transactions of the ASABE*, 42(1), 223–232. <https://doi.org/10.13031/2013.13199>

Peng, Y., Li, Z., Sun, T., Zhang, F., Wu, Q., Du, M., & Sheng, T. (2022). Modeling long-term water use and economic returns to optimize alfalfa–corn rotation in the Corn Belt of northeast China. *Field Crops Research*, 276, 108379. <https://doi.org/10.1016/j.fcr.2021.108379>

Putnam, D., Brummer, J., Cash, D., Gray, A., Griggs, T., Ottman, M., Riggs, W., Smith, M., Shewmaker, G., & Todd, R. (2020). *The importance of western alfalfa production*. Proceedings of the 29th National Alfalfa Symposium, Las Vegas, NV. National Alfalfa & Forage Alliance. <https://cales.arizona.edu/crop/counties/yuma/farmnotes/fn1101alfalfaprod.pdf>

Putnam, D. H., Gull, U., Radawich, J., Montazar, A., & Bali, K. (2018). Deficit irrigation strategies: Why alfalfa is the best crop to have in a drought. *Proceedings of the Second World Alfalfa Congress*, 49–53. <http://www.worldalfalfacongress.org/>

Quintero, D., Andrade, M. A., Cholula, U., & Solomon, J. K. Q. (2023). A machine learning approach for the estimation of alfalfa hay crop yield in Northern Nevada. *AgriEngineering*, 5(4), 1943–1954. <https://doi.org/10.3390/agriengineering5040119>

Raes, D., Fereres, E., García Vila, M., Curnel, Y., Knoden, D., Çelik, S. K., Uçar, Y., Türk, M., & Wellens, J. (2023). Simulation of alfalfa yield with AquaCrop. *Agricultural Water Management*, 284, 108341. <https://doi.org/10.1016/j.agwat.2023.108341>

Raes, D., Steduto, P., Hsiao, T. C., & Fereres, E. (2009). AquaCrop—The FAO crop model to simulate yield response to water: II. Main algorithms and software description. *Agronomy Journal*, 101(3), 438–447. <https://doi.org/10.2134/agronj2008.0140s>

Rotz, C. A., Corson, M. S., Chianese, D. S., Montes, F., Hafner, S. D., & Coiner, C. U. (2012). *The Integrated Farm System Model: Reference manual* (Version 3.6). USDA.

Robson, J. D., Armstrong, D., Cordell, J., Pope, D., & Flint, T. F. (2024). Calibration of constitutive models using genetic algorithms. *Mechanics of Materials*, 189, 104881. <https://doi.org/10.1016/j.mechmat.2024.104881>

Rymph, S. J. (2004). *Modeling growth and composition of perennial tropical forage grass* (Doctoral dissertation). University of Florida.

Saito, L., Freed, Z., Byer, S., & Schindel, M. (2022). The vulnerability of springs and phreatophyte communities to groundwater level declines in Oregon and Nevada, 2002–2021. *Frontiers in Environmental Science*, *10*, 1007114. <https://doi.org/10.3389/fenvs.2022.1007114>

Sanderson, M. A., Karnezos, T. P., & Matches, A. G. (1994). Morphological development of alfalfa as a function of growing degree days. *Journal of Production Agriculture*, *7*(2), 239–242. <https://doi.org/10.2134/jpa1994.0239>

Schreiber, M. M., Miles, G. E., Holt, D. A., & Bula, R. J. (1978). Sensitivity analysis of SIMED. *Agronomy Journal*, *70*(1), 105–108. <https://doi.org/10.2134/agronj1978.00021962007000010024x>

Soil Survey Staff, Natural Resources Conservation Service, U.S. Department of Agriculture. (2025). *Web soil survey*. <http://websoilsurvey.sc.egov.usda.gov/>

Steduto, P., Hsiao, T. C., Raes, D., & Fereres, E. (2009). AquaCrop—The FAO crop model to simulate yield response to water: I. Concepts and underlying principles. *Agronomy Journal*, *101*(3), 426–437. <https://doi.org/10.2134/agronj2008.0139s>

Stöckle, C. O., & Nelson, R. L. (1999). *CropSyst User's Manual*. Washington State University.

Strullu, L., Beaudoin, N., Thiébaud, P., Julier, B., Mary, B., Ruget, F., Ripoche, D., Rakotovololona, L., & Louarn, G. (2020). Simulation using the STICS model of C & N dynamics in alfalfa from sowing to crop destruction. *European Journal of Agronomy*, *112*, 125948. <https://doi.org/10.1016/j.eja.2019.125948>

Teuber, L. R., Taggard, K. L., Gibbs, L. K., McCaslin, M. H., Peterson, M. A., & Barnes, D. K. (1998). Fall dormancy: Standard tests to characterize alfalfa cultivars. *North American Alfalfa Improvement Conference*. <https://www.naaic.org/stdtests/>

Teshome, F. T., Bayabil, H. K., Schaffer, B., Ampatzidis, Y., Hoogenboom, G., & Singh, A. (2023). Exploring deficit irrigation as a water conservation strategy: Insights from field experiments and model simulation. *Agricultural Water Management*, *289*, 108490. <https://doi.org/10.1016/j.agwat.2023.108490>

Teixeira, E. I., Brown, H. E., Meenken, E. D., & Moot, D. J. (2011). Growth and phenological development patterns differ between seedling and regrowth lucerne crops (*Medicago sativa* L.). *European Journal of Agronomy*, *35*(1), 47–55. <https://doi.org/10.1016/j.eja.2011.03.003>

Thorp, K. R., Marek, G. W., DeJonge, K. C., & Evett, S. R. (2020). Comparison of evapotranspiration methods in the DSSAT Cropping System Model: II. Algorithm performance. *Computers and Electronics in Agriculture*, *177*, 105679. <https://doi.org/10.1016/j.compag.2020.105679>

United States Department of Agriculture, National Agricultural Statistics Service. (2025). *Crop production 2023 summary*. U.S. Department of Agriculture. <https://esmis.nal.usda.gov/sites/default/release-files/k3569432s/ns065v292/8910md644/cropan24.pdf>

U.S. National Integrated Drought Information System. (2025). *Colorado River drought contingency plan*. <https://www.drought.gov/colorado-river-drought-contingency-plan>

Wang, Y., Jiang, K., Shen, H., Wang, N., Liu, R., Wu, J., & Ma, X. (2023). Decision-making method for maize irrigation in supplementary irrigation areas based on the DSSAT model and a genetic algorithm. *Agricultural Water Management*, 280, 108231. <https://doi.org/10.1016/j.agwat.2023.108231>

Wang, Y., Sun, K., Gao, Y., Liu, R., Shen, H., Xing, X., & Ma, X. (2024). Improving crop model accuracy in the development of regional irrigation and nitrogen schedules by using data assimilation and spatial clustering algorithms. *Agricultural Water Management*, 291, 108645. <https://doi.org/10.1016/j.agwat.2023.108645>

Whitley, D. (1994). A genetic algorithm tutorial. *Statistics and Computing*, 4(2), 65–85. <https://doi.org/10.1007/BF00175354>

WRCC. (2021). *Station daily time series*. <https://wrcc.dri.edu/cgi-bin/rawMAIN2.pl?nvunrc>

Yang, S., Ge, Y., Wang, J., Liu, R., Tang, D., Li, A., & Zhu, Z. (2024). A dataset for estimating alfalfa leaf area and predicting leaf area index. *Frontiers in Plant Science*, 15, 1290920. <https://doi.org/10.3389/fpls.2024.1290920>

Zhang, N., Zhou, X., Kang, M., Hu, B.-G., Heuvelink, E., & Marcelis, L. F. M. (2023). Machine learning versus crop growth models: An ally, not a rival. *AoB Plants*, 15(2), plac061. <https://doi.org/10.1093/aobpla/plac061>

Zhao, R., Ma, Y., & Wu, S. (2024). A review of the research status and prospects of regional crop yield simulations. *Agronomy*, 14(7), 1397. <https://doi.org/10.3390/agronomy14071397>

Zhou, Z., Li, J., Gao, Y., Wang, X., Wang, R., Huang, H., Zhang, Y., Zhao, L., & Wang, P. (2024). Research on drought stress in *Medicago sativa* L. from 1998 to 2023: A bibliometric analysis. *Frontiers in Plant Science*, 15, 1406256. <https://doi.org/10.3389/fpls.2024.1406256>

Zumwald, M., Baumberger, C., Bresch, D. N., & Knutti, R. (2021). Assessing the representational accuracy of data-driven models: The case of the effect of urban green infrastructure on temperature. *Environmental Modelling & Software*, 141, 105048. <https://doi.org/10.1016/j.envsoft.2021.105048>

Appendix

Table 1: Definitions of cultivar and ecotype parameters used frequently throughout this thesis.

Parameters	Definitions
CSDL	Critical short-day length (h)
PPSEN	Relative response slope to photoperiod (1/h)
EM-FL	Light and heat time from seedling emergence to the appearance of the first flower (d)
FL-SH	Light and heat time from first inflorescence blooming to first inflorescence fruit setting (d)
FL-SD	The light and heat time from the first inflorescence blooming to the first inflorescence grain production (d)
SD-PM	Photothermal time from the first inflorescence grain to physiological maturity (d)
FL-LF	The light and heat time from when the first inflorescence blooms to when the leaves stop expanding (d)
LFMAX	Maximum leaf photosynthetic rate ($\text{mg CO}_2 \text{ m}^{-2} \text{ s}^{-1}$)
SLAVR	Specific leaf area under standard growth conditions ($\text{cm}^2 \text{ g}^{-1} \text{ DM}$)
SIZLF	Maximum blade size (cm^2)
RDRMT	Relative dormancy sensitivity to day length for partitioning (0-1)
RMRMM	Relative dormancy sensitivity to day length for mobilization (0-1)
TRIFL	Rate of appearance of leaves on the mainstem (leaves per thermal day)

Table 2: Genetic Algorithm operators used during calibration.

Parameter	Definition	In my script
num_generations	Number of evolutionary cycles (iterations).	GA repeats 100 iterations to improve parameters
sol_per_pop	Number of solutions in each generation (population size).	Each generation runs DSSAT 25 times
num_parents_mating	How many top solutions are chosen to create new offspring.	The 8 best parameter sets are chosen to create new ones.
num_genes	Number of parameters being optimized.	optimize 3 genes: LFMAX, TRIFL, RDRMT.
gene_space	Allowed range for each parameter (min-max values).	LFMAX (1.20-1.50), TRIFL (0.20-0.30), RDRMT (0.20-0.80). (Based on Literature)
fitness_func	A function that measures how good a solution is.	returns -RMSE for optimization.
mutation_num_genes	How many genes (parameters) are randomly changed in one new solution during mutation.	Mutates 1 parameter (gene) in each new offspring.
keep_elitism	The number of best solutions is preserved unchanged from one generation to the next.	Keeps 1 best solution from each generation (ensures progress).
parent_selection_type	The method the GA uses to pick which existing solutions will become parents.	"sss" (steady-state selection), the best solutions are chosen to mate and pass on their traits.
crossover_type	How the parents' genes are mixed to form offspring.	"single_point" splits the parameter list at one random point; one parent gives the first part, the other gives the rest.
mutation_type	The rule for generating new mutated values.	"random" the chosen gene's value is replaced with a new random value within its allowed min-max range.

Figure 1: Simulated versus observed alfalfa yield for the 2021 and 2022 growing seasons under full and deficit irrigation treatments before the first stage of calibration. Each point (2021) or cross (2022) represents an individual cut across both cultivars (Ladak II and Stratica). The 1:1 dashed red line indicates perfect agreement between observed and simulated yields.

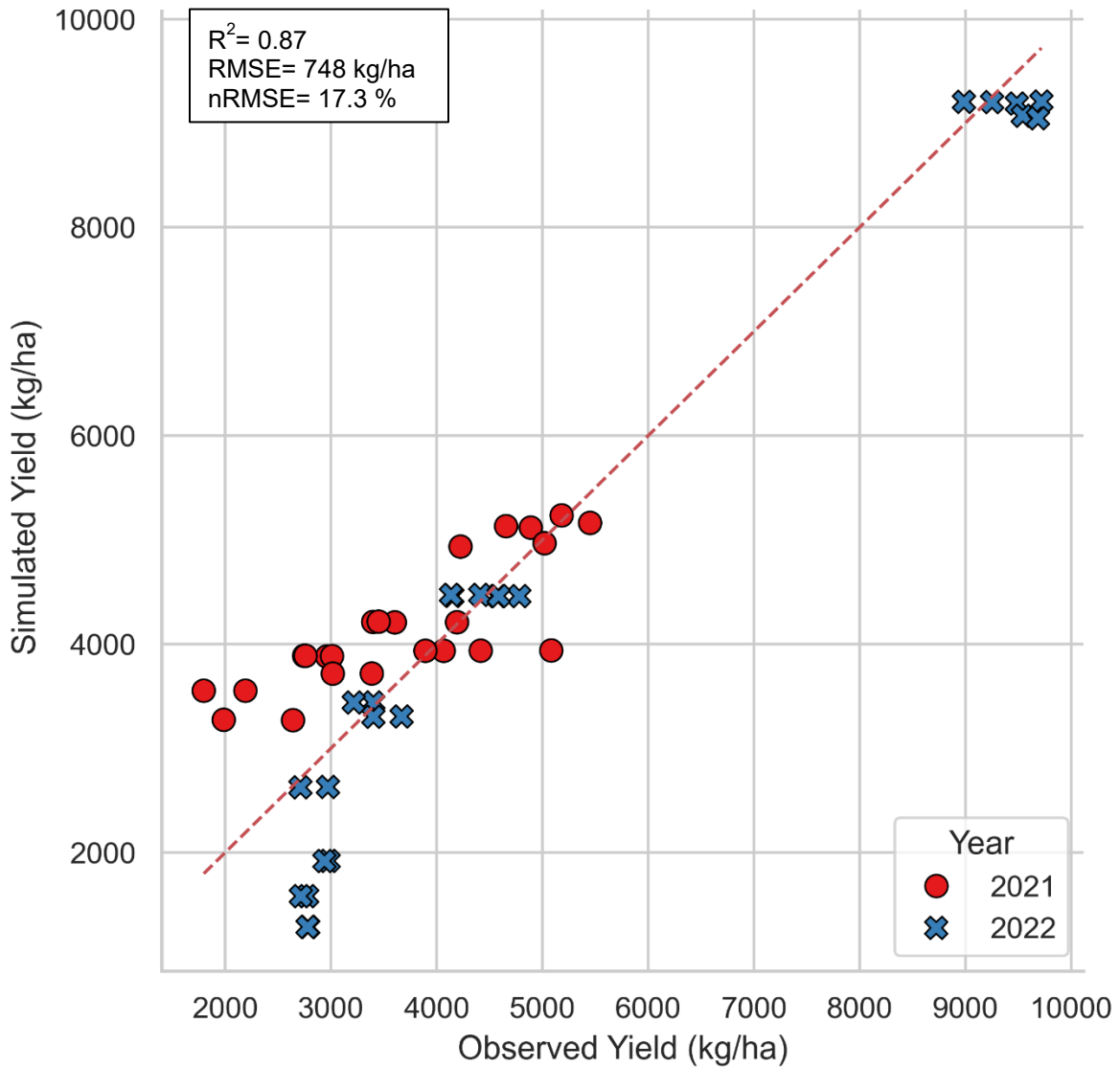


Figure 2: Simulated versus observed alfalfa yields for the 2023 evaluation year before stages of GA calibration. Each point (2023) represents an individual cut across both cultivars (Ladak II and Stratica) and three irrigation treatments. The 1:1 dashed red line indicates perfect agreement between observed and simulated yields.

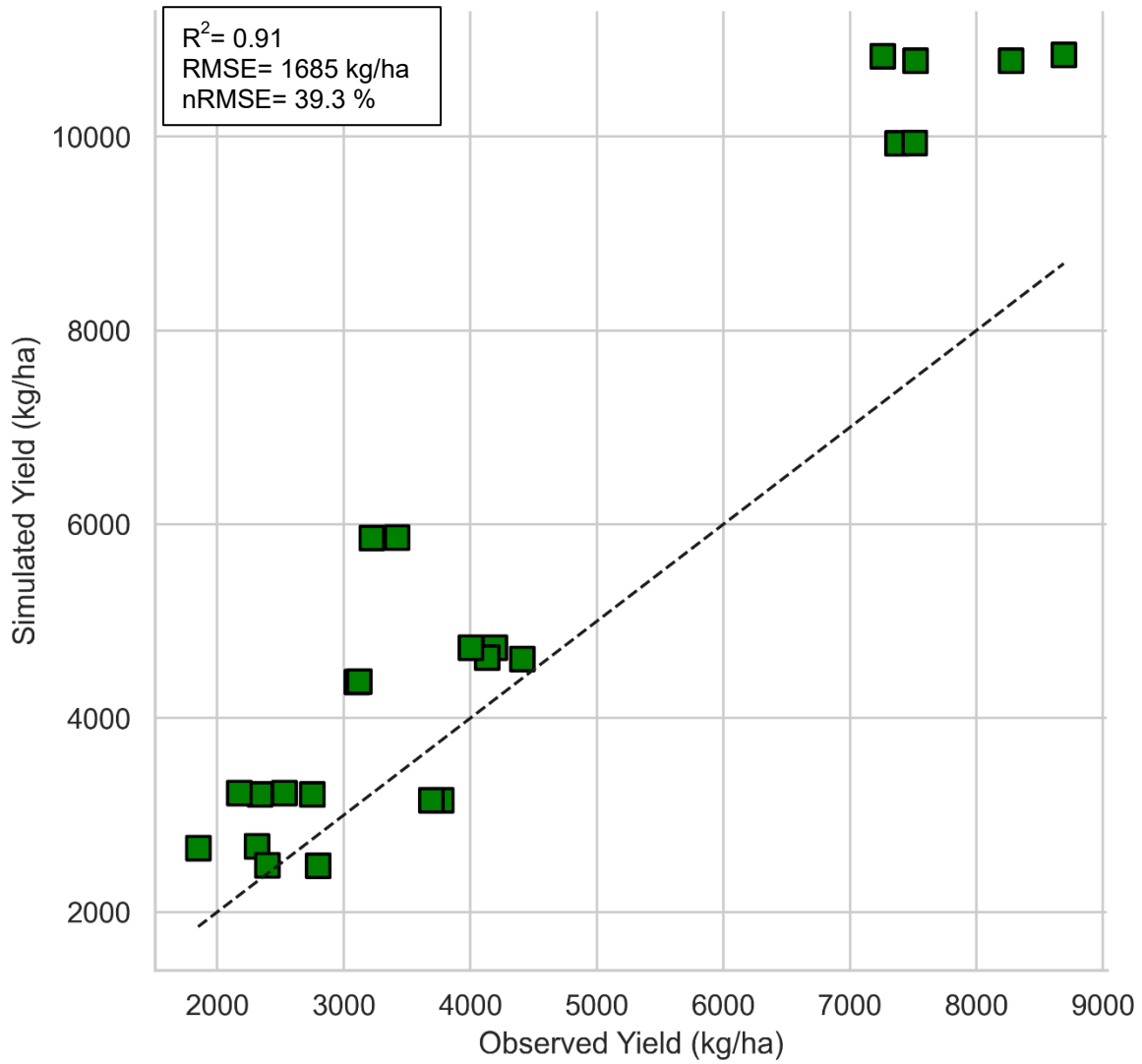


Figure 3: Simulated versus observed alfalfa yields for the 2023 evaluation year after the first stage of GA calibration. Each point (2023) represents an individual cut across both cultivars (Ladak II and Stratica) and three irrigation treatments. The 1:1 dashed red line indicates perfect agreement between observed and simulated yields.

